



# An integrated approach to the spatial distribution of the coastal infrastructure vulnerability by using coastal vulnerability index and hot spot analysis: a case study of Kusadasi-Selcuk

Tuncay Kuleli<sup>1</sup> · Seyma Bayazit<sup>1</sup>

Received: 8 March 2024 / Accepted: 16 June 2024  
© The Author(s) 2024

## Abstract

In this study, a new methodology integrating spatial coastal vulnerability index (CVI) and hot spot analysis was proposed for a comprehensive and holistic coastal infrastructure (natural, built-up and socioeconomic) vulnerability assessment and determination of its spatial distribution. The Selçuk-Kuşadası coastal region, which is located on the Aegean coast of Turkey, was chosen as the case study area. For calculation spatial CVI, eight physical variables (geomorphology, coastal slope, relief, mean seal level, mean tide range, mean wave high, shoreline erosion and accretion) were used. Spatial CVI analyses were performed using basic methods of geographical information systems. CVI results were classified as 1 to 5 across the study area. The spatial distribution of vulnerabilities of coastal infrastructures has statistically tested with hotspot analysis. In conclusion; over 55% of infrastructure falls within high or very high vulnerability classes. It is seen that 57% of the infrastructure in the build-up category, 59% of the natural environment, and more than 42% of the socio-economic infrastructure are located in areas falling into the high or very high vulnerability classes. Additionally, \$1.1 billion worth of land assets and a population of approximately 143.000 people are located in areas that fall into the high or very high vulnerability classes. Statistically significant clusters of high vulnerability for historical sites, tourism, roads, land value, population density, and urban areas were determined by hot spot analysis. According to the results of the developed integrated method, suggestions were presented for the preparation of coastal infrastructure vulnerability adaptation strategies.

**Keywords** CVI · Hot spot · Infrastructure · Coastal zone · GIS

---

✉ Tuncay Kuleli  
tuncaykuleli@mu.edu.tr  
Seyma Bayazit  
seymabayzit@mu.edu.tr

<sup>1</sup> Bodrum Maritime Vocational School, Mugla SK University, Bodrum, Mugla, Turkey

# 1 Introduction

Sea level rise (SLR) is recognized as a global problem that can cause serious environmental and socio-economic challenges, particularly in coastal environments, as highlighted by the 6th Assessment Report of the International Panel on Climate Change (IPCC), which predicts a rise to 2 m by 2100 under the very high greenhouse gas emission scenario (SSP5-8.5) due to deep uncertainty regarding ice sheet processes (IPCC 2023; IPCC 2022; IPCC 2021). It is emphasized that the possibility of the approaching and rising above 15 m in 2300 should not be ignored (IPCC 2023). For every centimetre of SLR, thousands of hectares of land would be lost on the land side of the shoreline (Lewsey et al. 2004). Moreover, the relative SLR, which includes land subsidence, seems likely to reach 1 m well before 2150 in the most densely populated coastal areas and 4 m in the coming centuries (Vernimmen 2023). Additionally, the population density within 150 km of the coast is currently at approximately 44% of the world's population, with expectations of a 25% increase by 2050 (Zhao et al. 2022).

The low elevation coastal zone (LECZ) in the world covers 2.3% of the total surface area of the coastal countries, and while 625.2 million people lived in the LECZ regions of the world in 2000, it is estimated that this population will reach between 879.1 and 948.9 million in 2030 and between 1052.8 and 1388.2 million in 2060 (Neumann et al. 2015). Coastal areas are vulnerable to SLR due to its effects such as coastal flooding, coastal erosion, saltwater intrusion, rising coastal water, submergence of low-lying wetlands and dry land, loss of coastal habitats, degradation of coastal ecosystems, storm damage due to its rising frequency and intensity (Lewsey et al. 2004; Wang and Marsooli 2021). It is estimated that the population living in coastal areas, social structure, economic structure, coastal ecosystems and coastal infrastructures will increasingly continue to be negatively affected by the threats arising from SLR (Tang et al. 2013; Rani et al. 2015; Shen et al. 2016; Wang and Marsooli 2021).

The acceleration of SLR amplifies the cumulative impact on coastal communities, and scientific endeavours, particularly in coastal vulnerability research, appear to be increasing in order to reduce risks and secure the continued existence of vulnerable populations (Bukvic 2020; Sarkar 2022; Minunno 2023). Existing research on coastal vulnerability primarily employs four methods: index-based, indicator-based, GID-based decision support systems, and dynamic computer models (Pethick and Crooks 2000; Rani et al. 2015; Ramieri et al. 2011; Dey and Mazumder 2023). There is a consensus that the coastal vulnerability index (CVI) is the most effective, straightforward, and commonly used quantitative method to assess coastal vulnerability to SLR (Djouder and Boutibal 2017; Koroglu et al. 2019; Fernandez-Macho et al. 2020; Lopes et al. 2022; Kovaleva et al. 2022).

The foundation of the CVI method, which is widely used in coastal vulnerability research, was laid by Gornitz (1990) (Fernandes-Macho 2020, Kovelava et al. 2020; Beeharry et al. 2022). It is an index-based semi-quantitative method that is used to assess the relative vulnerability of coastal areas to climate change, particularly to SLR associated hazards such as erosion and inundation (Gornitz 1990, 1991; Gornitz and White 1992; Gornitz et al. 1994). Thieler and Hammar-Klose (2000) modified the initial CVI index which was developed by, resulting in it being a useful tool that utilized across various territorial scales. Numerous modified CVI formulations have been proposed, integrating additional physical variables to better represent specific coastal areas. An appreciable number of coastal vulnerability

researches have then utilized the CVI method (Lewsey et al. 2004; Mani Murali 2013; Tang et al. 2013; Rani et al. 2015; Behera et al. 2019; Wang and Marsooli 2021; Beeharry et al. 2022; Kovaleva et al. 2022; Dey and Mazumder 2023; Charuka et al. 2023). Most of these researches used remote sensing and geographical information systems GIS tools (Rani et al. 2015). While the CVI and its modifications, utilize physical variables to assess SLR impacts (Koroglu et al. 2019; Fernandez-Macho et al. 2020), recent research emphasizes the need to integrate socio-economic factors (Mani Murali et al. 2013; Rani et al. 2015; Shen et al. 2016). One of the first studies to evaluate physical and socio-economic variables together is Boruff et al. (2005). Various others modified the index by including socio-economic variables of the coastal areas (Mani Murali et al. 2013; Shen et al. 2016; Djouder and Boutiba 2017; Behera et al., 2019; Koroglu et al. 2019; Charuka et al. 2023; Dey and Mazumder 2023). Most researches utilize the standart CVI formulation and classify the result using 1–5 scale (very low to very high vulnerability) (Koroglu et al. 2019; Dey and Mazumder 2023). However, some of them expand the CVI method by adding analytic hierarchy process (AHP) (Mani Murali et al. 2013; Rani et al. 2015; Charuka et al. 2023). In addition, there are methodological differences in the selection of the study area to be analysed for coastal vulnerability. Some have determined a linear buffer zone up to a certain distance from the coastline, such as 0.5 km, 5 km from the coastline (Rani et al. 2015; Kantamaneni 2016; Behera et al. 2019), while others used administrative borders such as district or neighbourhood borders (Charuka et al. 2023). However, when boundaries are determined statically, such as administrative boundaries or a selected buffer zone, especially in studies that integrate the CVI with social dimension, this may reduce the accuracy of the analyses (Mani Murali et al. 2013). Furthermore, a notable gap in prior research lies in the absence of statistical reliability testing for the distribution of coastal vulnerability across the studied area (Koroglu et al. 2019). Still, The CVI methodology remains a widely accepted approach for identifying vulnerable coastal areas, guiding further investigation and adaptation planning (Koroglu et al. 2019; Lopes et al. 2022).

Although there is much research on coastal vulnerability, a few focus on coastal infrastructure vulnerability due to SLR (Kantamaneni 2016; Shen et al. 2016). Some studies have focused on coastal infrastructure vulnerability but most of their examinations were based on flood scenarios (Tang et al. 2013; Shen et al. 2016). However, there is still a limited understanding of how the relationship between sea level rise and the impact on coastal infrastructure affects society's adaptation response. Nazarnia et al. (2020) encouraged researchers to develop integrated assessment methods for making urban systems, such as coastal infrastructures (roads, water, and power lines, etc.), resilient to the effects of SLR. Charuka et al. (2023) also stressed the importance of the determination of the areas with high vulnerability using integrated methods for the investment of coastal defence infrastructure.

Considering the gaps in the literature, a new methodology that integrates a spatial CVI analysis into the coastal infrastructure (natural, built and socioeconomic) for a comprehensive and holistic coastal vulnerability assessment was proposed in this study. The study area is Selcuk-Kusadasi, which has a unique natural, historical, cultural, and economic value and is located in the Aegean coasts of Turkey. For the assessment of coastal infrastructure vulnerability across the study area, coastal vulnerability level of each grid calculated using the Gornitz (1990)'s CVI formula. To do this, eight physical variables (geomorphology, coastal slope, relief, mean seal level, mean tide range, mean wave hight, shoreline erosion and accretion) were used and the data obtained from different sources. The spatial CVI

analyses performed by basic GIS methods (subset, buffer, slope, reclass, map algebra etc.), CVI results showed the vulnerability levels from 1 (very low) to 5 (very high) across the study area. The study area boundary was redefined by removing areas with CVI-1 to make a dynamic, more realistic, and time-saving assessment. Natural (cropland, wetland etc.), built (coastal infrastructures such as ports, roads, tourism sites etc.), and socioeconomic (population density, land price etc.) infrastructures of study area were determined according to quality, quantity and location information and a geographical database was created. The spatial distribution of coastal vulnerabilities of different types of coastal infrastructures was obtained. Finally, the statistical reliability test of the distribution of the coastal infrastructures across the area with different vulnerability level was examined via hot spot Analyses, for the first time in this study. Findings provided not only the distribution of vulnerable coastal infrastructures but also their patterns formed in some locations with different levels of vulnerability. This study proposes a novel integrated approach that combines spatial Coastal Vulnerability Index (CVI) analysis with the assessment of natural, built, and socioeconomic infrastructure across the Kusadasi-Selcuk region in Turkey. This approach aims to overcome limitations in existing methods by providing a more comprehensive and spatially explicit understanding of coastal infrastructure vulnerability to SLR, ultimately informing the development of targeted adaptation strategies for vulnerable areas.

## 2 Study area

Kusadasi-Selcuk coastal area, located in the Aegean Sea of Turkey, is a dynamic and versatile coastal region characterized by its natural beauty, historical significance, urban development, and a combination of various economic activities (Fig. 1). Although tourism and related industries dominate the economic landscape in the study area, other sectors such as agriculture and manufacturing also maintain their importance (KCoC 2015; SCoC 2015). The Kusadasi-Selcuk coastal region, situated on the Aegean coast of Turkey, is characterized by a varied coastline encompassing sandy beaches and rocky cliffs (Kahraman 2011). Kusadasi, a city with a population of 130,835 (TURKSTAT 2023) and an area of 264 km<sup>2</sup> (MoEUCC 2023), boasts a thriving tourism sector alongside agriculture and manufacturing (KCoC 2015). Its natural beauty, historical significance, and proximity to cultural heritage sites like Ephesus contribute to its popularity as a summer tourism destination.

Selcuk, with a population of 38,151 in the year 2022 (TURKSTAT 2023) and an area of 295 km<sup>2</sup> (SCoC 2015), hosts a significant portion of the cultural and natural assets that make Kusadasi an important tourism city. Notable attractions in Selcuk include the ancient city of Ephesus (UNESCO World Heritage), the Temple of Artemis, the House of the Virgin Mary, and various other cultural sites (SCoC 2016). Tourism-related sectors play a vital role in Selcuk's economy, alongside agricultural activities (SCoC 2015). The study area is well-connected by various modes of transport, including highways (Izmir-Selcuk), railways (Selcuk-Çamlık stations on Izmir-Aydın line), air travel (Izmir's Adnan Menderes Airport and Selcuk's Efes Airport), and maritime transport (Kusadasi port and marina). Given the coastal morphology, historical and cultural assets, and spatial distribution, it's understood that the Kusadasi and Selcuk coastal areas need to be studied as a whole. Therefore, the coastal boundary within the study area has been defined as the approximately 67 km stretch of coastline between Karasu Bay within Dilek Peninsula National Park in the south and

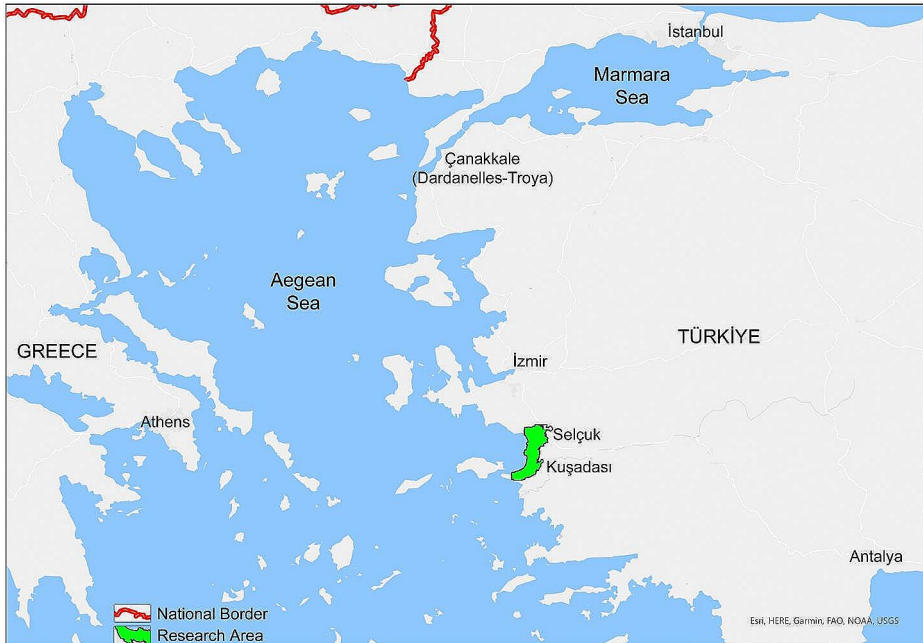


**Fig. 1** Kusadasi-Selcuk coastal region as case study area

Yoncaköy Beach located at the northern end of Pamucak Beach. The Kusadasi-Selcuk case study provides a microcosm where broader theoretical frameworks and practical solutions can be developed. The selection of Kusadasi-Selcuk as a study area is thought to be aligned with the research objectives and methodology. Coastal vulnerability, intertwined socio-economic framework, cultural heritage, and global representation converge to provide a research field that enriches the depth and applicability of the study.

### 3 Data and methods

The data, data sources and methodologies used to achieve the research objectives was described in this section. The collection and preparation of data along with the methods used to obtain meaningful insights and achieve the purpose of the research was given in detail. This section is divided into two subheadings: Data and Method. The information and data used is detailed in the Data subheading, and the approaches and methods used are explained in the Method subheading.

#### 3.1 Data

In this study, the data used were organized into two main categories. The first category pertains to the dataset used to calculate the CVI. This dataset encompasses the key variables required for calculating the CVI, which is a significant metric for the vulnerability index. The second category includes the dataset used to assess the vulnerability of build-

up infrastructures, natural environment infrastructures, and socio-economic infrastructure using CVI classes, and hot spot analysis. The data and data sources used in this research and which form the basis of our study were comprehensively presented in Table 1. The Table 1 encompasses a comprehensive set of variables that were utilized to assess both the coastal vulnerability index and the vulnerability of coastal infrastructure in the study area.

*Coastal Slope and relief:* Derived and extracted through processing from the Shuttle Radar Topography Mission (SRTM) dataset (NASA JPL 2013; SRTM 2018). The SRTM dataset provides elevation data with a horizontal resolution of approximately 30 m for most of the world, making it one of the highest quality global digital elevation models (DEM) available.

*Relative Sea Level Change:* Relative sea level change data ( $3.3 \pm 1.1$  mm/yr) was obtained from various sources (Kuleli 2010; TUDES 2022; SLE 2022; Caldwell 2015; Zlotnicki et al. 2019; CMS 2021).

*Shoreline Erosion/Accretion:* Shoreline erosion/accretion rates were determined using the Digital Shoreline Analysis System (DSAS) on Sentinel-2 imagery (ESA 2023) from 2018 to 2023, along with digitized shorelines from Google Earth (2014). This approach allowed us to calculate End Point Rate (EPR) values in meters/year for coastal erosion and accretion areas.

*Mean Tide Range:* Data for mean tide range, which falls within the range of study area, was sourced from TUDES (2022), Sayre et al. (2021), Sayre et al. (2018), and ECU (2022).

*Mean Wave Height:* Mean wave height data, range in the study area, and was collected from various sources, including Özhan and Abdalla (2002), CMS (2022), Sayre et al. (2021), Sayre et al. (2018), and ECU (2022).

*Landuse/Landcover:* Information on landuse/Landcover (LC/LU) was derived from the CORINE Coastal Zone 2018 dataset and Akbaş et al. (2011). CORINE Coastal Zone 2018 dataset is a specialized subset of the larger CORINE dataset, focusing specifically on land cover and land use information in coastal regions of Europe. The CORINE Coastal Zone 2018 dataset typically maintains a spatial resolution of around 100 m. The CORINE dataset was developed to support environmental policy planning and decision-making at regional, national, and European levels. It categorizes the Earth's surface into more than 40 land cover classes, including forests, urban areas, agriculture, wetlands, water bodies, and more.

*Geology:* Geological data was extracted from Geoscience Map Viewer presented at the Mineral Research and Exploration (MTA) of the Directorate General and Akbaş et al. (2011). Further details can be found at <http://yerbilimleri.mta.gov.tr/Default.aspx>.

*Urban, Cropland, Woodland and Forest, Grassland, Heathland and Scrub, Open Space with Little or No Vegetation, Wetland, Water, Build-up Area, Settlements:* Extracted from the CORINE Coastal Zone LC/LU and the Global Human Settlement Layer (GHSL) dataset available at [https://ghsl.jrc.ec.europa.eu/ghs\\_buS2023.php](https://ghsl.jrc.ec.europa.eu/ghs_buS2023.php).

*Leisure, Amenity, Historic, Roads, Public Transport, Tourism:* The classification scale made by Open Street Map (OSM) according to these “key values” was used. Data sourced from OSM and [https://wiki.openstreetmap.org/wiki/Main\\_Page](https://wiki.openstreetmap.org/wiki/Main_Page).

*Land Square Meter Unit Price* Information on land square meter unit prices was gathered from e-Government Gateways of various municipalities, including Kusadasi, Selcuk, Tire, Torbali, Menderes, and Soke. Land Square Meter Unit Price is a value that is determined every year by the Municipality and shows only the land price. This value does not include the monetary value of infrastructure and superstructure.

**Table 1** The data and data sources

Variables ( $a_n$ )	Data source
To calculate CVI	Data sources
V1 Coastal slope	Processing from Shuttle Radar Topography Mission (SRTM) dataset
V2 Relief	From SRTM (NASA JPL, 2013; SRTM, 2018)
V3 Relative sea level change	3.3 ± 1.1 mm/yr from Kuleli (2010), TUDES (2022), SLE (2022), Caldwell (2015), Zlotnicki et al.(2019), CMS (2021)
V4 Shoreline erosion / accretion	-1 - +1 m/yr from Sentinel-2 images from Copernicus, 10 m resolution and Google Earth
V5 Mean tide range	(0.15–0.16) 0.2–0.3 m from TUDES (2022), Sayre et al. (2021), Sayre et al. (2018), ECU (2022)
V6 Mean wave height	(0.62) 1.1–2.0 m from Özhan and Abdalla (2002), CMS (2022), Sayre et al. (2021), Sayre et al. (2018), ECU (2022)
V7 Landuse/Landcover	CORINE 2018 Akbaş et al. (2011)
V8 Geology	Akbaş et al. (2011)
To evaluate coastal infrastructure	Data sources
Land Cover: CLC	CORINE (2018) Coastal Zone LC/LU
Urban	
Cropland	
Woodland and Forest	
Grassland	
Heathland and Scrub	
Open space with little or No Vegetation	
Wetland	
Water	
Build-up Area	Pesaresi and Politis (2023) GHSL - Global Human Settlement Layer,
Settlements	GHS built-up surface grid
Leisure	<a href="https://www.openstreetmap.org">https://www.openstreetmap.org</a>
Amenity	<a href="https://wiki.openstreetmap.org/wiki/Main_Page">https://wiki.openstreetmap.org/wiki/Main_Page</a>
Historic	
Roads	
Public Transport	
Tourism	
Land square meter unit price	e-Government Gateway Kusadasi Municipality: <a href="https://www.turkiye.gov.tr/kusadasi-belediyesi-arsa-rayic">https://www.turkiye.gov.tr/kusadasi-belediyesi-arsa-rayic</a> e-Government Gateway Selcuk Municipality: <a href="https://www.turkiye.gov.tr/selcuk-belediyesi-arsa-rayic-degeri-sorgulama">https://www.turkiye.gov.tr/selcuk-belediyesi-arsa-rayic-degeri-sorgulama</a> e-Government Gateway Tire Municipality: <a href="https://www.turkiye.gov.tr/tire-belediyesi-arsa-rayic-degeri-sorgulama">https://www.turkiye.gov.tr/tire-belediyesi-arsa-rayic-degeri-sorgulama</a> e-Government Gateway Torbali Municipality: <a href="https://www.turkiye.gov.tr/torbali-belediyesi-arsa-rayic-degeri-sorgulama">https://www.turkiye.gov.tr/torbali-belediyesi-arsa-rayic-degeri-sorgulama</a> Menderes Municipality: <a href="https://e-belediye.menderes.bel.tr/ebelediye/SorgulamaIslemleri/ArsaRayicDegerleri">https://e-belediye.menderes.bel.tr/ebelediye/SorgulamaIslemleri/ArsaRayicDegerleri</a> Soke Municipality: <a href="https://odeme.soke.bel.tr/web/guest/5">https://odeme.soke.bel.tr/web/guest/5</a>
Population	<a href="https://www.nufusune.com/kusadasi-ilce-nufusu-aydin">https://www.nufusune.com/kusadasi-ilce-nufusu-aydin</a>
Population density	Obtained by processing the neighbourhood polygon map and the neighbourhood population

*Population:* Population data were obtained from Turkish Statistical Institute (TUIK) on the basis of neighbourhoods included in the study area. from <https://www.nufusune.com>.

*Population Density* Population density was determined through processing neighbourhood polygon maps and neighbourhood population data.

### 3.2 Methods

The research methodology was presented through a flowchart shown in Fig. 2. This flowchart summarizes the sequence of methodological steps applied in the study and provides an overview of the methodological framework used in our research.

In this study, a five-step methodological approach was applied;

- Dynamic boundary detection to determine the border on the land side of the coast in the study area,
- Selection variables for CVI calculation and selection coastal infrastructure classes. Converting data obtained from different sources into GIS geo-database,
- Calculation of CVI values (GIS based analyses),
- Determining the spatial distribution and quantities of infrastructures within areas with CVI values (GIS based analyses),
- Hot Spot Analysis for Reliability. Determining the distribution of infrastructures within areas with CVI values according to their statistical importance.

#### 3.2.1 Determining the dynamic boundary on the land side and CVI grid size of the study area

There is no generally accepted standard size for the grid sizes used in CVI analyses. Grid sizes used in research vary depending on the size and scale of the study area. While in some studies the grid size is preferred as 500 m, in some studies it can be 1 km or more (Gzam et al. 2006; Hegde and Reju 2007; Torresan et al. 2008; Abuodha and Woodroffe 2010; Hastuti et al. 2022.; Šimac et al. 2023). In this research, SRTM 30 m grid size, which is used for elevation and slope analysis, was preferred for CVI analyses. On the other hand, there is no generally accepted standard distance for the landward border of the coast for areal CVI analyses. In some studies, the limit on the land side of the coast is preferred as 1 km, while in other studies, 250–500 m is preferred (Mullick et al. 2019; Meddah et al. 2023; Roukounis et al. 2023; Rani et al. 2015; Kantamaneni 2016; Behera et al. 2019). This study adopted a novel approach to define the landward boundary for CVI analysis. Instead of relying on a fixed distance, we delineated a dynamic boundary based on the elevation data. Specifically, we considered the area up to 30 m above the land elevation, which is a key CVI variable. This approach offers several advantages compared to the traditional fixed distance method. Firstly, it accounts for the diverse coastal geomorphology and topography of the study area, ensuring a more accurate representation of the landward extent potentially vulnerable to coastal hazards. Secondly, using a set elevation provides objectivity and standardization, eliminating the subjectivity associated with choosing a specific fixed distance. Instead of a fixed distance, using the land elevation up to 30 m allows for a dynamic boundary that adapts to the specific topography of the coastline. This can capture the nuanced variations





in vulnerability due to local slopes and elevations, which could provide a more accurate assessment.

### 3.2.2 Selection variables for CVI calculation and selection coastal infrastructure classes. Converting data obtained from different sources into GIS geo-database

According to the CVI classes in Table 2, the methods for acquiring each variable utilized in the calculation of the CVI were explained in the following paragraphs.

*Coastal Slope:* The coastal slope variable was derived from the SRTM dataset using the following Eq. 1 (Young 2022);

$$\%Slope = \frac{\Delta h}{\Delta d} \times 100 \tag{1}$$

The coastal slope was calculated using the difference in elevation between two points divided by the horizontal distance separating them. Where Δh corresponds to rise, which is

**Table 2** The percentage breakdown of infrastructures classified under different Coastal Vulnerability Index classes for the regions of Kusadasi and Selcuk

Variable	Unit	Ranking of Coastal Vulnerability Index Variables				
		Very Low 1	Low 2	Moderate 3	High 4	Very High 5
<b>1 Coastal slope</b> (Lopez et al. 2016)	%	>12	8–12	4–8	2–4	<2
<b>2 Relief</b> (Gornitz 1991)	m	>30	21–30	11–20	6–10	0–5
<b>3 Relative sea level change</b> (Gornitz 1991)	mm/yr	<-1	-1.0-0.9	1.0–2.0	2.1-4.0	>4.0
<b>4 Shoreline erosion / accretion</b> (Gornitz 1991)	m/yr	>2.0	1.0–2.0	-1 - +1	-1.1 - -2.0	<-2.0
<b>5 Mean tide range</b> (Gornitz 1991)	m	<1.0	1.0-1.9	2.0–4.0	4.1-6.0	>6.0
<b>6 Mean wave height</b> (Thieler and Hammar-Klose 2000)	m	<1.1	1.1-2.0	2.0-2.25	2.25–2.60	>2.60
<b>7 Landuse/ Landcover</b> (Satta et al. 2015)		Bare areas	Shurupland, grasslands, sparse vegetation	Forest	Agriculture	Urban and industrial infrastructure
<b>8 Geology</b> (Gornitz 1991)		Plutonic, volcanic, high-medium grade metamorphics	Low grade metamorphics, sand-stones and conglomerates, metamorphics rocks	Most sedimentary rocks	Coarse, poorly sorted, unconsolidated sediments	Fine, consolidated sediment, ice

the change in elevation (vertical distance) between two points, and  $\Delta d$  corresponds to run, which is the horizontal distance between those two points. The slope map was reclassified according to the ranges of CVI values in Table 2, and a new slope raster image consisting of values ranging from 1 to 5 was obtained. Flatter slopes, indicating higher vulnerability to erosion, were assigned higher CVI scores according to the classification in Table 2.

*Relief:* The Relief variable represents the elevation of coastal land, indicating the variation in height above sea level. The elevation data was derived from the SRTM dataset. The SRTM coastal land elevation data was reclassified based on predefined ranges, as delineated in Table 2.

*Relative sea-level change:* The raw data obtained from the sources outlined in Table 1, which pertains to relative sea level change, was transformed into a raster format. The raster data representing relative sea level change was reclassified based on the CVI ranges detailed in Table 2. Post-reclassification, a raster image was generated, showing the CVI categories between 1 and 5 to relative sea level change.

*Shoreline Erosion / accretion:* To detect erosion and accretion on the shoreline, 176 transects perpendicular to the shoreline, 500 m long, 250 m apart, were created using the Digital Shoreline Analysis System (DSAS) software. The DSAS is a free software designed for the quantitative analysis of coastal changes based on digitized shoreline data and it facilitates the examination of shoreline dynamics, erosion, and accretion patterns, offering a comprehensive toolset for researchers and coastal management professionals (Himmelstoss et al. 2021). The calculation of the End Point Rate (EPR) involves dividing the distance of shoreline movement by the temporal interval between the oldest and most recent shoreline data points. The EPR is favoured for its computational simplicity and minimal reliance on merely two shoreline dates (Himmelstoss et al. 2021). A shoreline dataset including baseline, transect, and shoreline and intersect data was used to calculate the relationship between shoreline change statistics.

*Mean Tide Range:* The raw data obtained from the sources outlined in Table 1, which pertains to mean tide range, was transformed into a raster format. The raster data representing mean tide range change was reclassified based on the CVI ranges detailed in Table 2. Post-reclassification, a raster image was generated, showing the CVI categories between 1 and 5 to mean tide range change.

*Mean Wave Height:* The raw data obtained from the sources outlined in Table 1, which pertains to mean wave height, was transformed into a raster format. The raster data representing mean wave height change was reclassified based on the CVI ranges detailed in Table 2. Post-reclassification, a raster image was generated, showing the CVI categories between 1 and 5 to mean wave height.

*Landuse/Landcover:* The landform variable refers to the physical characteristics of the land surface within the coastal zone. It plays a crucial role in determining the vulnerability of a particular area to erosion and inundation due to sea level rise. Some common landform examples include; bare areas, shrubland, grasslands, sparse vegetation, forest, agriculture, urban and industrial infrastructure. Each landuse type is assigned a score within the CVI framework, ranging from 1 to 5. The higher vulnerability scores are assigned to landforms with low elevation, gentle slopes, and unconsolidated sediments, while lower scores are assigned to landforms with higher elevation, steeper slopes, and more resistant materials.

*Geology:* Geology is another important variable within the CVI calculation, providing insights into the long-term evolution and composition of the coastal landscape. Each geo-

morphic feature type is assigned a score within the CVI framework (Table 2), reflecting its inherent vulnerability to sea level rise and associated coastal hazards. More resistant features like bedrock coasts receive lower vulnerability scores, while features prone to erosion or flooding receive higher scores.

### 3.2.3 Calculation of CVI values

The second phase entails the preparation of the CVI variables. The CVI approach, a key component of this study, is widely used as an index-based methodology for determining coastal vulnerability related to sea-level rise. Many of the CVI methods commonly employed for assessing vulnerability in coastal zones have their roots in the work of Gornitz (1990, 1991), who conducted comprehensive evaluations of the United States coastline on a national scale, as noted by Koroglu et al. (2019). Subsequently, Shaw et al. (1998) and Gornitz (1991) incorporated the geology variable into CVI calculations, enhancing the index's precision. Following the selection and preparation of CVI variables, CVI values were calculated using the following equation (Gornitz 1991);

- $a_1$ : Coastal slope.
- $a_2$ : Relief.
- $a_3$ : Relative sea level change.
- $a_4$ : Shoreline erosion / accretion.
- $a_5$ : Mean tide range.
- $a_6$ : Mean wave height.
- $a_7$ : Landform.
- $a_8$ : Geomorphology

$$CVI = \sqrt{\frac{a_1 \times a_2 \times a_3 \times a_4 \times \dots \times a_n}{n}} \quad (2)$$

Each variable ( $a_1$  to  $a_8$ ) was assigned a score between 1 and 5 based on its vulnerability class as defined in Table 2. The current analysis assigns standard formula and equal weight to all CVI variables. The sum of these scores represents the CVI value for each grid cell within the study area. CVI values were then classified into five categories based on their vulnerability levels, as outlined in Table 2;

- CVI 5: Very high (Red or dark red).
- CVI 4: High (Orange).
- CVI 3: Moderate (Yellow).
- CVI 2: Low (Green or light green).
- CVI 1: Very Low (Dark green).

### 3.2.4 Determining the spatial distribution and quantities of infrastructures within areas with CVI values

The CVI results were transformed from a raster image into vector polygons, with each polygon categorized by its corresponding CVI value (1–5) using the raster to polygon process. Using the attribute selection process, we separated the newly created vector polygons based on their CVI value. This allowed us to analyse infrastructure within each CVI class indepen-

dently. Finally, the polygon-line-point intersect process was applied. This overlaid each CVI class polygon onto its corresponding infrastructure dataset. By doing this, we identified all infrastructure components located within each CVI zone, enabling further analysis of their vulnerability based on their location and surrounding CVI value.

***Hot spot analysis for reliability. determining the distribution of infrastructures within areas with CVI values according to their statistical importance:***

This research employed hot spot analysis (Getis-Ord  $G_i^*$ ) to reveal spatial patterns in coastal infrastructure vulnerability. This technique identifies statistically significant clusters of high or low vulnerability within spatial data. Rooted in spatial autocorrelation principles (Getis and Ord 1992, 2010; Ord and Getis 1995), it unveils pronounced clustering beyond visual inspection. Our aim was to delineate areas with concentrated vulnerability exceeding random expectations. hot spot analysis provides Z-scores and p-values for cluster significance. Z-scores indicate standard deviations from the mean, with positive values denoting high values surrounded by similar values (hot spots) and negative values indicating low values surrounded by similar values (cold spots) (Esri 2023a, b). Larger magnitudes imply stronger clustering.

P-values measure evidence against random spatial patterns (Esri 2023a, b). Small p-values ( $<0.05$ ) suggest statistically significant non-random patterns, while large p-values suggest potential randomness. Therefore, a significant positive Z-score with a small p-value identifies a hot spot, while a significant negative Z-score with a small p-value indicates a cold spot. Non-significant results suggest random chance might explain the observed pattern. This analysis prioritizes intervention and adaptation strategies, directing resources to areas with elevated coastal infrastructure risks. This analysis informs the prioritization of intervention and adaptation efforts, efficiently directing resources toward areas facing elevated coastal infrastructure risks.

## 4 Results

The research findings and results were given across three subsections. Firstly, the distributions of the eight CVI variables and the spatial patterns of the calculated CVI classes were presented through maps and graphs. Secondly, the results regarding the amount and spatial distribution of infrastructures within areas corresponding to CVI values were explained. These results have allowed for a better understanding of how the infrastructures were distributed concerning their vulnerability. Thirdly, reliability results were given showing the distribution of infrastructures within CVI areas according to their statistical significance with hot spot analysis. These assessments have provided information about the statistical significance of the spatial distribution of infrastructure vulnerability.

*Spatial distribution of CVI variables:* The coastline length in the case study area where CVI classes and variables were calculated was approximately 67 km. The size of the area for which spatial CVI values were calculated was approximately 247km<sup>2</sup>. This area covers a dynamic region from the coastline to where the CVI-2 border ends and the CVI-1 border begins on the land side. The CVI-1 value means very low vulnerability and extends to distant inland areas not spatially related to the coast.

*Slope variations:* As can be seen from the map in Fig. 3(a), the majority of the coastal area in the Kusadasi-Selcuk region falls into the CVI-5-4-3 categories, which means that

it is Moderate to High Vulnerable. In particular, Pamucak (Efes) Beach, which is approximately 9 km long, and the Kucuk Menderes delta located behind this beach, have a very flat slope and continue up to a distance of approximately 22 km on the land side. In addition, Kusadasi district centre and the 13 km coastal area located to the south of the district centre are also in the CVI-5 class, a large area with a very flat slope. However, there are also some areas in the CVI-1 and CVI-2 categories, which means that they are Very Low and Low Vulnerable. These areas are mainly located in the high flatlands near the coast and the mountainous parts of the hinterland, respectively.

*Relief- elevation variations:* Similar to the slope distribution, in the same places, as can be seen from the map in Fig. 3(b), the majority of the coastal area in the Kusadasi-Selcuk region falls into the CVI-5-4-3 classes in terms of the spatial distribution of land elevation, which means that it is Moderate to Very High Vulnerable. The areas with the highest elevations (CVI-1 and CVI-2) are located further inland.

*Relative sea level change variations:* The map in Fig. 4(a) shows that the relative sea level change in the Kusadasi-Selcuk coastal region varies between 3.02 mm/yr and 3.24 mm/yr from north to south. This range of relative sea level change falls within CVI-4 class (High Vulnerability). Areas classified as CVI-4 in terms of relative sea level change are more likely to be adversely affected by sea level rise than areas with lower CVI classes.

*Shoreline erosion / accretion variations:* The map in Fig. 4(b) shows that there is a lot of variation in shoreline erosion/accretion rates along the Kusadasi-Selcuk coast. Some areas are experiencing erosion, while others are accreting. The rates of erosion and accretion vary from  $-1.0$  m per year to  $+1.8$  m per year. The map shows that the shoreline in the Kusadasi-Selcuk region is mostly in the CVI-2 and CVI-3 classes, which means that it is low to moderately vulnerable to erosion. The minimum erosion rate is  $-1.0$  m/yr, which falls within the range of CVI-3 (Moderate Vulnerable). However, the maximum accumulation rate is  $+1.8$  m/year, and although it exceeds the upper limit of CVI-3, it does not fall within the lower limit of CVI-2. Therefore, CVI class was accepted as 3 (Moderate Vulnerability) for shoreline erosion/accretion ratio.

*Mean tide range variations:* Analysis of the literature presented in Table 1 reveals a mean tide range of 0.2–0.3 m within the study area, characterizing microtidal conditions. This value aligns with the CVI-1 (Very Low) classification scheme (Fig. 4(c)).

*Mean wave height variations:* Based on the literature reviewed in Table 1, the mean wave high variable within the study area exhibits values ranging from 1.1 to 2.0 m, indicative of low wave energy conditions. This value corresponds to the CVI-2 (Low) classification scheme (Fig. 4(d)).

*Landuse/Landcover variations:* The map in Fig. 3(c) shows that the majority of the Kusadasi-Selcuk coastal region is covered by agriculture. There is also a significant amount of urban and industrial infrastructure along the coast. The forested areas are mainly located in the hills and mountains to the north and east of the coastal plain. The large amount of agricultural land means that the region is at risk of erosion and flooding. The urban and build-up infrastructure along the coast is also at risk of damage from storms and sea level rise. The forested areas in the hills and mountains can help to protect the coast from erosion, but they are also at risk of wildfires.

*Geology variations:* The map in Fig. 3(d) shows that the geology of the coastal region is varied, with a mix of different types. The most vulnerable areas are the fine, sand dune, consolidated and unconsolidated sediments, which are classified as CVI-5 and are shown

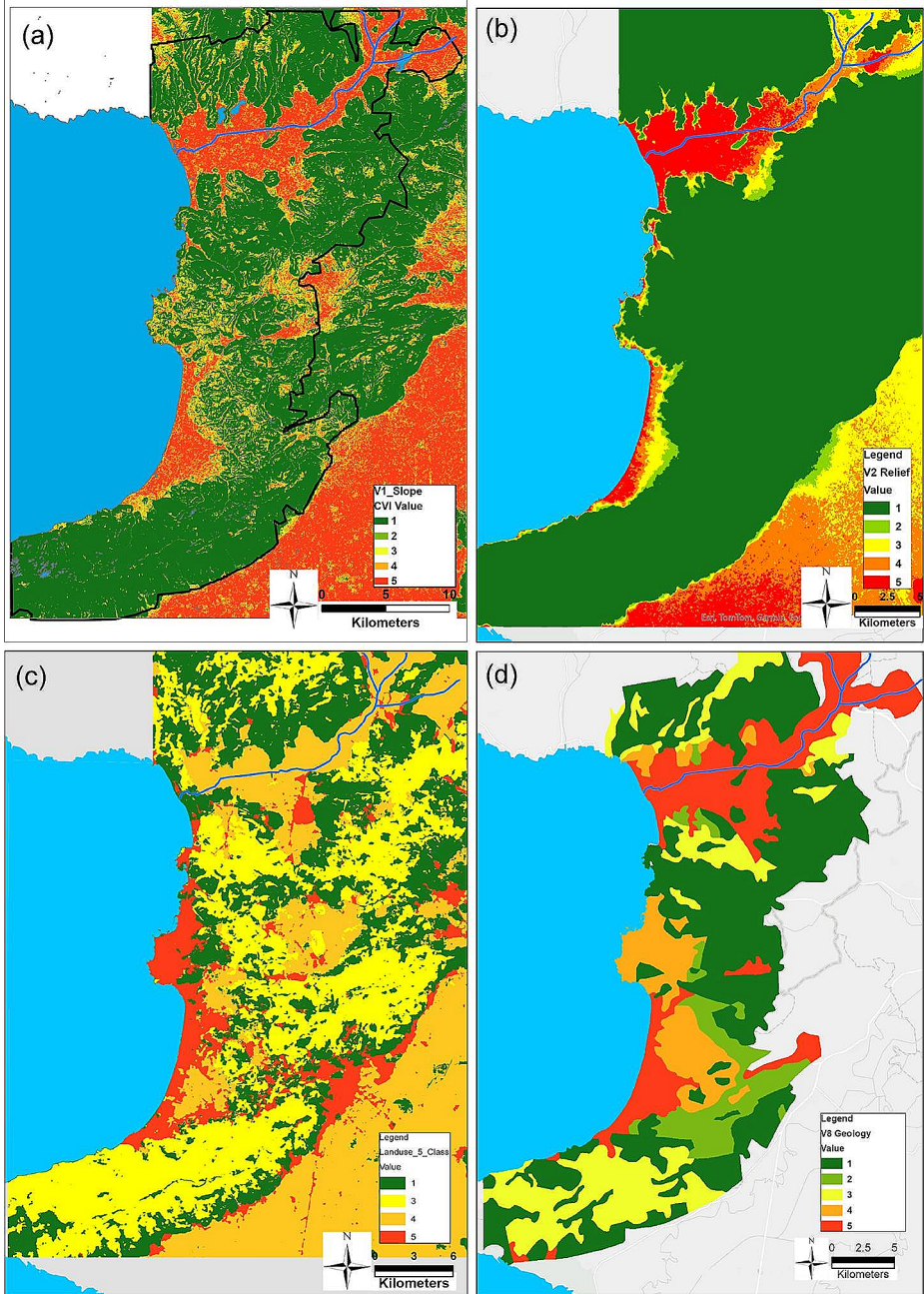
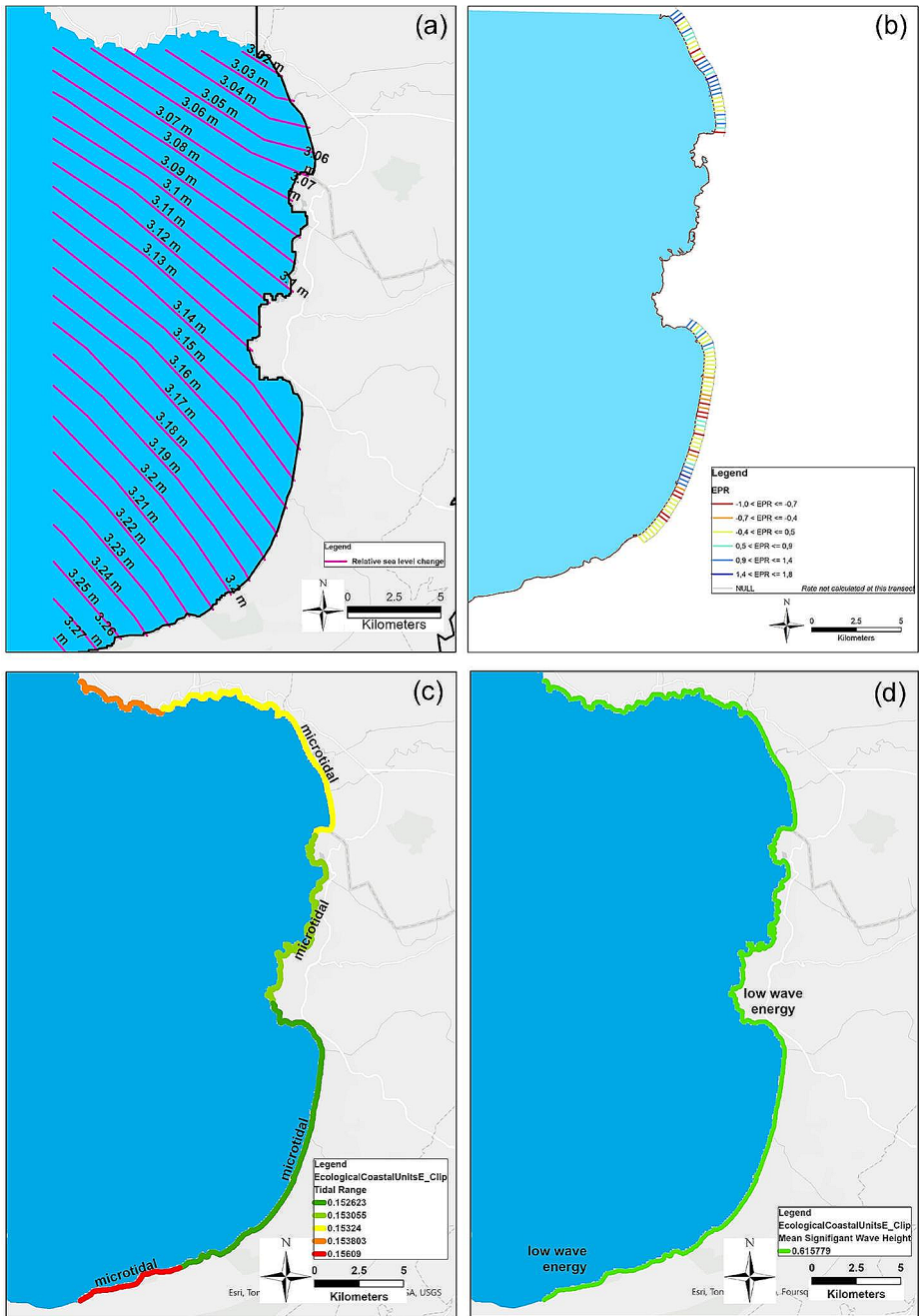


Fig. 3 CVI classes of slope (a), elevation (b), landuse/Landcover (c) and geology (d) variables



**Fig. 4** CVI classes of relative sea level change (a), shoreline erosion/accretion (b), mean tide range (c) and mean wave height variables



in red on the map. The least vulnerable areas are the plutonic, volcanic, and high-medium grade metamorphic rocks, which are classified as CVI-1 and are shown in dark green on the map. The most common rock types are sedimentary rocks, which are classified as CVI-3 and are shown in yellow on the map.

*CVI variations:* As can be seen from the pie chart in Fig. 5 and map in Fig. 6, it was determined that the total area classified as CVI 5 accounted for 35%, while CVI 4 covered 13%, CVI 3 comprised 15%, and CVI 2 represented 37%.

The map in Fig. 7 shows that the most vulnerable places in the Selcuk region, on the northern side of the study area, against sea level rise are the Kucuk Menderes River delta and the low-lying areas around Pamucak (Ephesus) Beach which is about 9 km length. Kucuk Menderes delta and its wetland, which starts from Pamucak (Ephesus) beach, is a low-lying area with a length of approximately 22 km on the land side and a width of 7 km in some places, and a very large area in this region is seen to have CVI of 5, which means they are very highly vulnerable. Another highly vulnerable area on the north side, indicated by CVI 4 to 5 values, is concentrated around the district centre of Selcuk and the Ephesus Ancient city. This is because these areas are low-lying, have gentle slopes, and are made

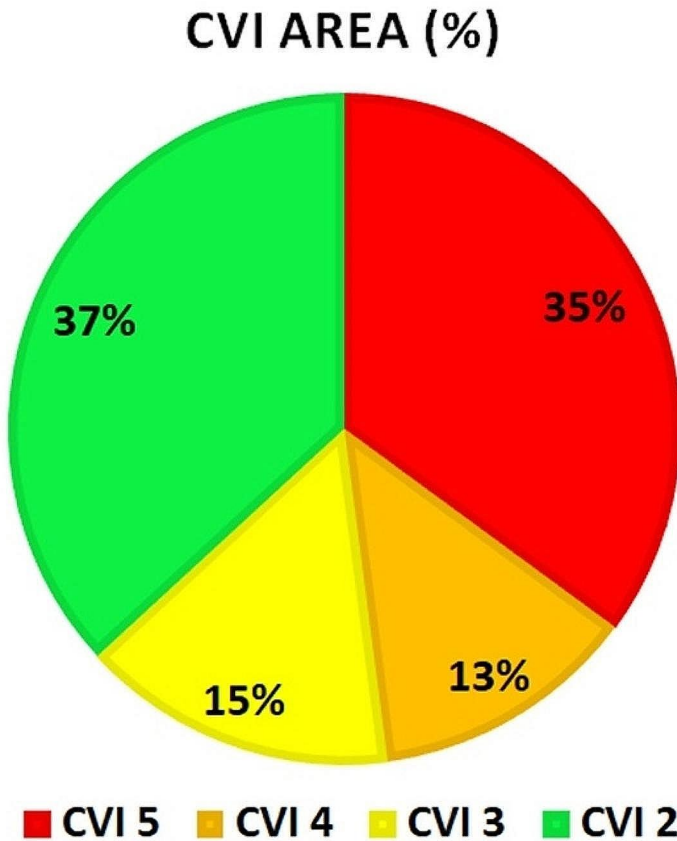


Fig. 5 Spatial distribution of CVI classes in percentage

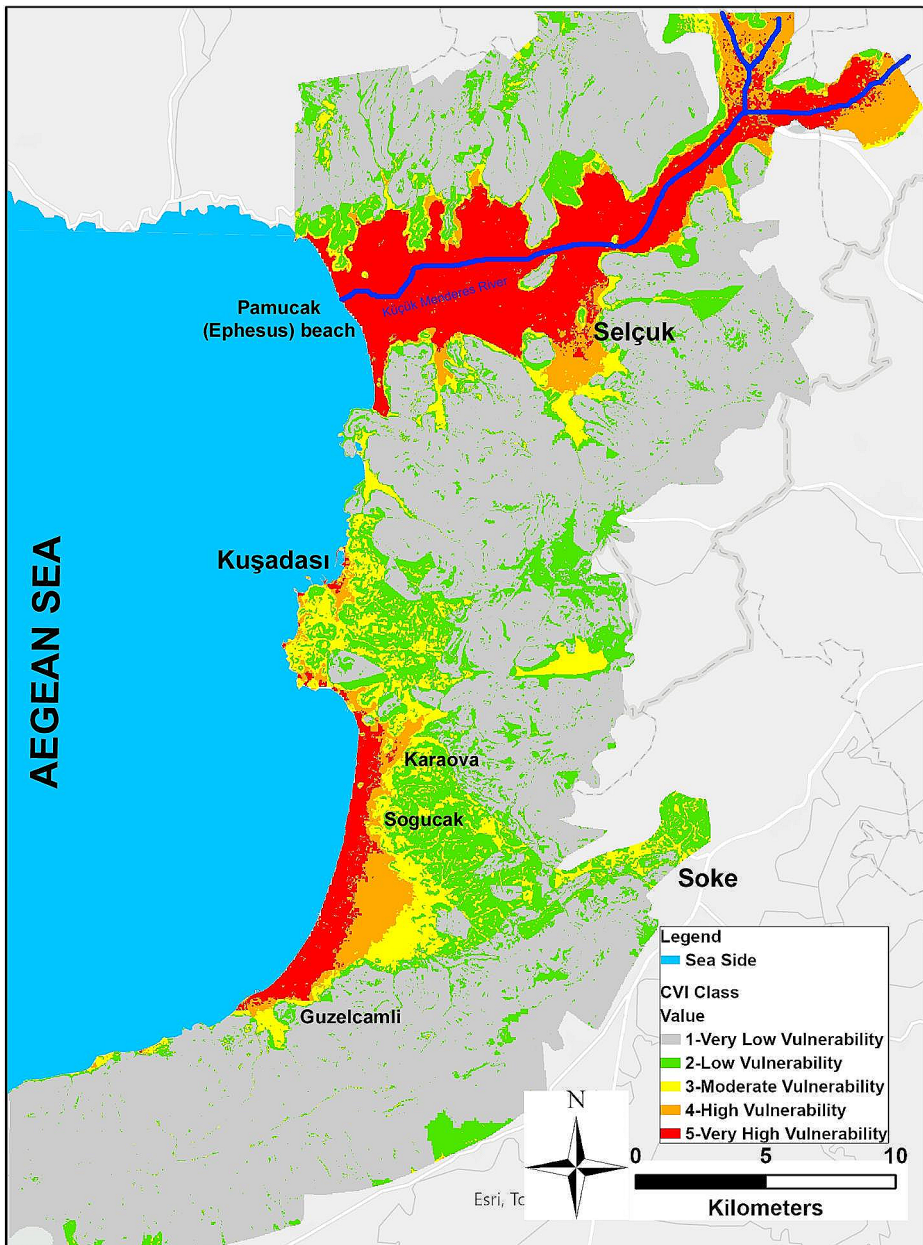
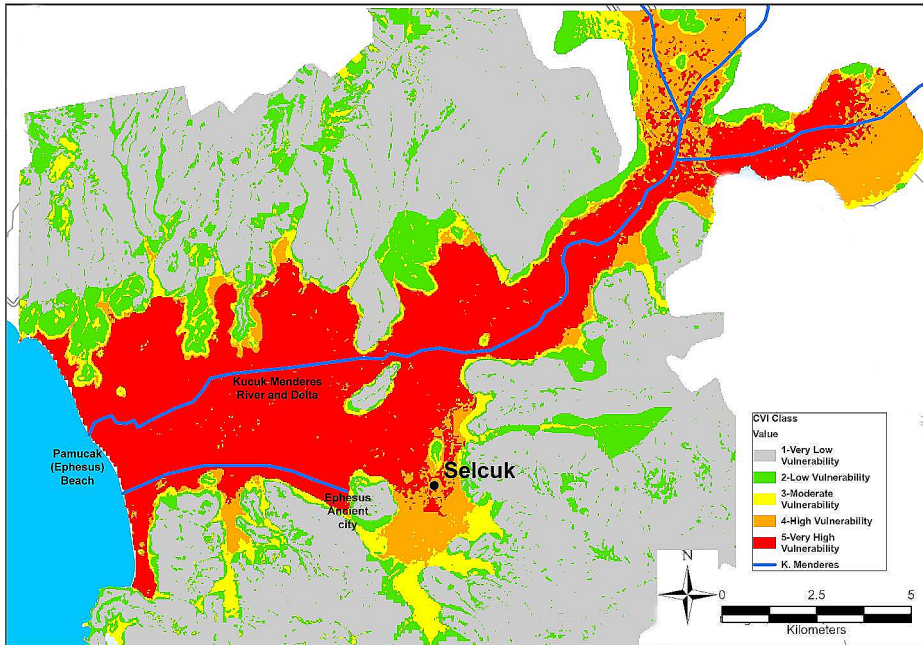


Fig. 6 Spatial distribution of CVI classes

up of sandy sediments. The map shows that the most vulnerable areas (CVI-5, red) are the delta of the Kucuk Menderes River and the area around Pamucak Beach. These areas are low-lying and have sandy soils, which makes them more vulnerable to SLR.



**Fig. 7** Spatial distribution of CVI classes in Selcuk region

The Selcuk town-district centres and Ephesus Ancient City are also in areas with relatively high CVI values (CVI-4 and CVI-5). These areas are more likely to be damaged by SLR, coastal storms and flooding. The map also shows the location of the Kucuk Menderes River and its delta. The river is a major source of sediment for the Selcuk coast, and its delta is an important area for wildlife. The delta is also a relatively vulnerable area, as it is low-lying and has sandy soils. The areas with the lowest CVI values (CVI-1 and CVI-2, light green) are the areas along the coast that are protected by cliffs or other natural barriers such as high elevation. These areas are less vulnerable to SLR and other coastal hazards. Overall, the map shows that the Selcuk coastal region is a relatively vulnerable area to SLR and other coastal hazards. The most vulnerable areas are the delta of the Kucuk Menderes River and the area around Pamucak Beach. The Selcuk district centres and Ephesus Ancient City are also in areas with relatively high CVI values.

The map in Fig. 8 shows that the Kusadasi district centre, located in the southern part of the study area, was also determined as CVI-4 and 5 (High and Very High). This is because some parts of the city are built on reclaimed land and are close to the sea. Some important areas in the district centre, especially the marina, cruise port and the famous Ladies Beach, are at a very high vulnerability level. It has been determined that the areas around Guzelcamli, Sogucak and Karaova, located further south of the Kusadasi district centre, have CVI-5 and 4 (High and Very High) values. These regions are more vulnerable because the land elevation is lower and the slopes are flatter. However, this region, which is in the CVI-5 class and where the second houses and pedestrian roads are located, has a coastline of approximately 13 km and a width of 1.5 km in some places on the land side.

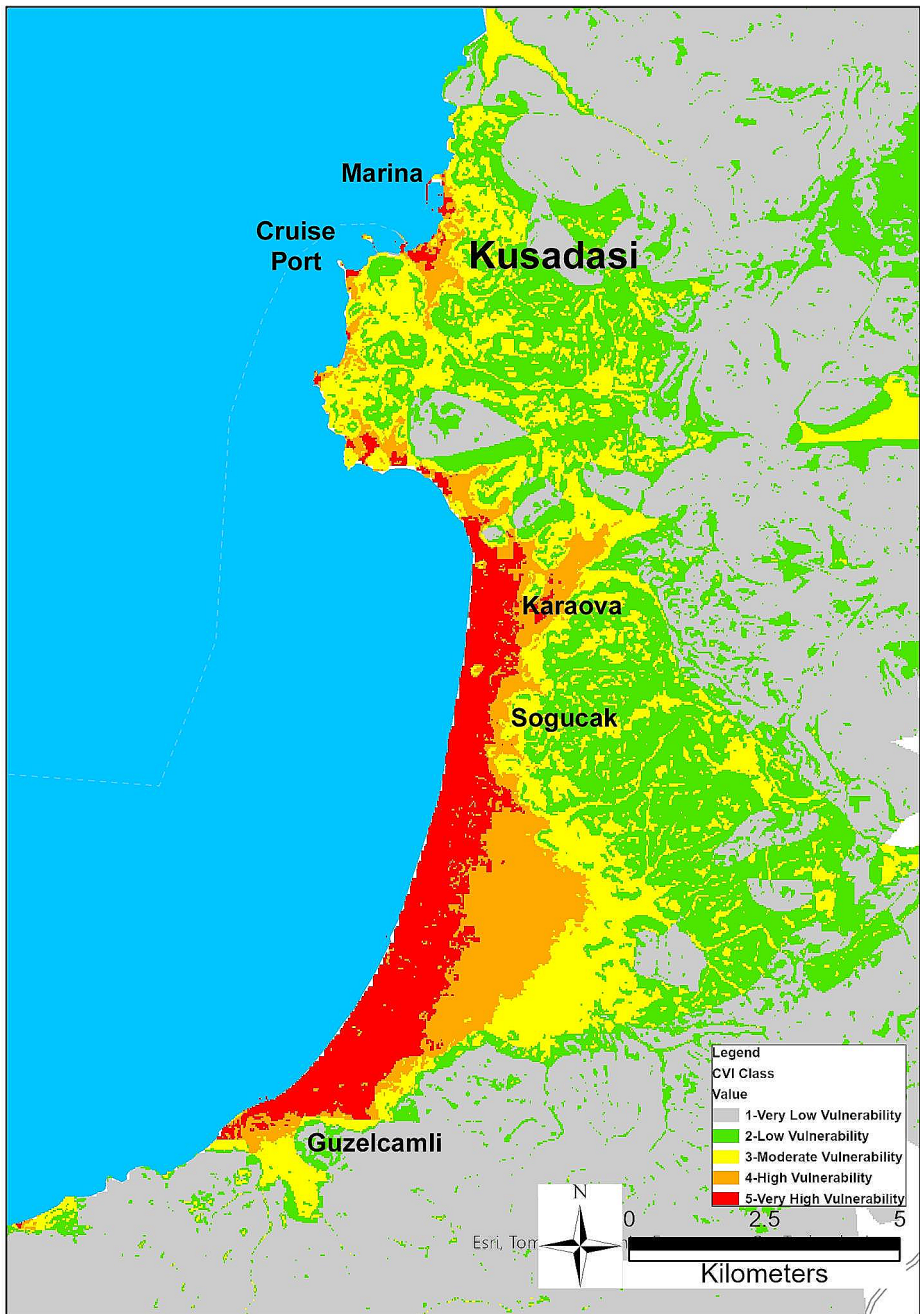


Fig. 8 Spatial distribution of CVI classes in Kusadasi region

*The spatial distribution of infrastructure vulnerability within areas with CVI values:* In this section, the analysis identified varying vulnerability levels within Kusadasi and Selcuk infrastructure across different CVI zones (Fig. 9).

The percentage breakdown of infrastructures under different CVI classes for the Kusadasi and Selcuk was presented in Table 3. Over 41% of the total infrastructure falls within the very high vulnerability class (CVI 5), signifying a remarkable risk from coastal hazards. While high vulnerability (CVI 4) infrastructure accounts for 13.84%, the combined percentage of highly vulnerable infrastructure reaches a worrying 55%. Conversely, only 17.34% and 27.66% of the infrastructure are classified as moderate vulnerability (CVI 3) and low vulnerability (CVI 2), respectively.

The infrastructures within the CVI-5 class had the highest rates in Kusadasi and Selcuk. These include leisure facilities, historical sites, roads, tourism-related infrastructures, urban build-up areas, cropland areas, wetland areas, water bodies, open spaces with little or no vegetation, and the distribution of total infrastructure. Leisure facilities (71.43%) were the most vulnerable within the CVI-5 class. This can be attributed to their proximity to coastal areas, making them vulnerable to coastal hazards such as erosion and storm surges. Historical sites (44.44%) were also significantly vulnerable. Their cultural and historical importance makes them valuable assets, but their location near the coast exposes them to risks associated with sea level rise. Roads (29.94%) were another infrastructure category highly vulnerable to coastal hazards. As vital transportation networks, they could be exposed to the impacts of erosion and flooding, which can disrupt connectivity and mobility. Tourism-related infrastructures (29.23%) include hotels, resorts, and recreational facilities that attract visitors to the coastal areas. Due to their proximity to the coast, they face risks from sea-level rise, storms, and other coastal hazards, which can negatively impact tourism activities. Urban build-up areas (33.48%) and cropland areas (37.75%) also exhibited considerable vulnerability. Their proximity to the coast makes them vulnerable to flooding and erosion, affecting urban development and agricultural activities. Wetland areas (90.84%), water bodies (94.34%), and open spaces with little or no vegetation (91.64%) had the highest vulnerability rates within the CVI-5 class. These ecosystems provide valuable ecological services but are highly vulnerable to coastal hazards due to their location along the coast.

Moving to the CVI-4 class, infrastructures with the highest rates were amenity facilities (38.08%) and population density (28.59%). These factors indicate that areas with higher population density and amenities face relatively higher vulnerability to coastal hazards.

Within the CVI-3 class, public transportation infrastructures (42.86%) had the highest rates. This suggests that transportation systems, such as buses or trains, face significant vulnerability, potentially impacting the movement of people in coastal areas. In the CVI-2 class, Woodland and Forest areas (81.88%), Grassland areas (49.72%), and Heathland and scrub areas (69.89%) exhibited the highest rates of vulnerability. These natural ecosystems are critical for biodiversity and provide valuable ecosystem services. However, their vulnerability to coastal hazards, such as erosion and inundation, can have severe ecological consequences.

An analysis of the spatial distribution of CVI for land square meter unit price was conducted to estimate the monetary value of land within different CVI classes. This approach effectively expresses the vulnerability in terms of potential economic losses. Applying the CVI to land values, a monetary distribution was generated. This analysis aimed to estimate the economic significance of varying vulnerability levels. Within the CVI class 5 (highest

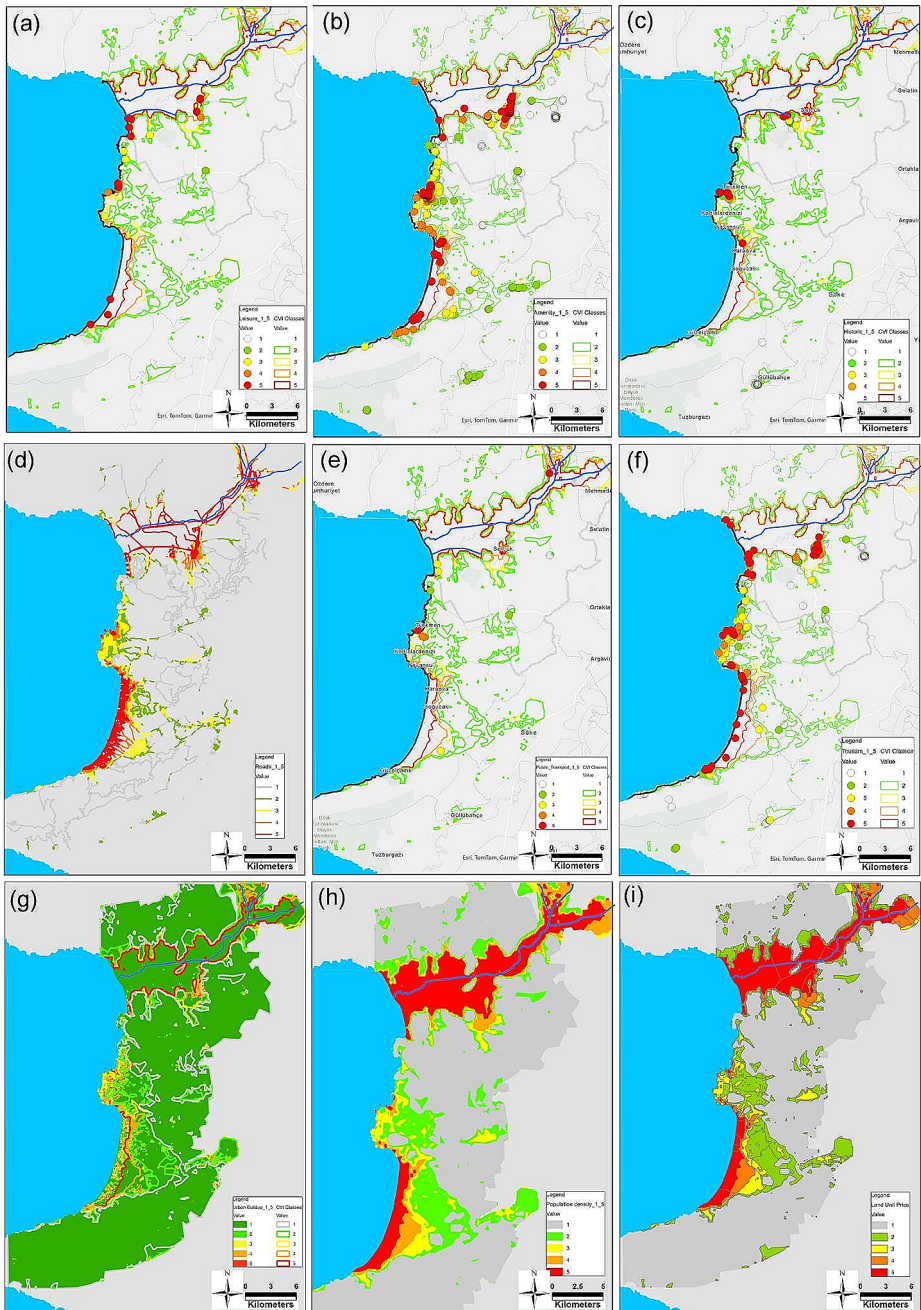


**Fig. 9** The spatial distribution of infrastructures within different CVI classes; leisure (a), amenity (b), historic (c), roads (d), public transport (e), tourism (f), urban, build-up area (g), population density (h) and land square meter unit price

**Table 3** CVI variables and classes

No	Infrastructure	CVI 5	CVI 4	CVI 3	CVI 2	
1	<b>Build-Up</b>	Leisure	71.43	14.29	14.29	0.00
2		Amenity	32.56	38.08	16.28	13.08
3		Historic	44.44	7.41	14.81	33.33
4		Roads	29.94	16.96	28.61	24.49
5		Public Transport	21.43	21.43	42.86	14.29
6		Tourism	29.23	28.46	24.62	17.69
7		Urban - Buildup Area	33.48	11.87	26.77	27.88
8		Cropland	37.75	17.89	14.07	30.29
1	<b>Natural</b>	Woodland and Forest	2.80	3.56	11.77	81.88
2		Grassland	33.64	5.08	11.55	49.72
3		Wetland	90.84	6.00	2.47	0.69
4		Water	94.34	4.01	1.44	0.21
5		Heathland and scrub	13.46	4.39	12.26	69.89
6		Open spaces with little or no vegetation	91.64	1.71	1.90	4.75
1	<b>Socio-economic</b>	Population Density	24.17	28.59	24.14	23.10
2		Land Square Meter Unit Price	19.60	12.50	21.63	46.28
	<b>Distribution of Total Infrastructure</b>		41.16	13.84	17.34	27.66

vulnerability), representing 19.6% of the land area, the monetary value (USD \$) reached approximately \$660.7 million. Similarly, class 4 (high vulnerability) held 12.5% of the land area, translating to a monetary value of roughly \$421.3 million. Class 3 (medium vulnerability), encompassing 21.63% of the land, was valued at \$729.1 million. Notably, the combined value of land classified as very high (CVI-5) and high vulnerability (CVI-4) reached approximately \$1.08 billion. These findings highlight the varying levels of vulnerability for different infrastructures within each CVI class. Understanding these vulnerabilities is important for effective adaptation strategies in Kusadasi and Selcuk.

*Hot Spot Analysis results for reliability. The distribution of infrastructures within areas with CVI values according to their statistical importance:* in this section, the spatial distribution of hot spot results of infrastructures in the study area was provided with a detailed overview. Hotspots (areas with statistically significant high CVI values) are concentrated near Kusadasi (north), Selcuk (south), and the Aegean Sea (west). Conversely, cold spots (low vulnerability) are found centrally and in the east.

An analysis of the map in Fig. 10(b) shows numerous hot spots with high CVI values, signifying areas where historical sites have more vulnerability. Hot spots of high vulnerability for historical sites are concentrated in the north (Kusadasi) and central areas (Selcuk) compared to the south.

Figure 10(c, d) shows leisure and public transport infrastructure throughout Kusadasi-Selcuk. Unlike other features, vulnerability for these areas is scattered (no red/blue clusters). This means vulnerability varies across these sectors, requiring custom solutions rather than location-specific interventions.

Figure 10(e) shows tourism areas vulnerable to coastal hazards (red/pink) along the west and north coastlines of Kusadasi and Selcuk. These areas likely contain hotels, restaurants, and recreational facilities at high risk. Cold spots (blue) in the east and south indicate lower vulnerability.

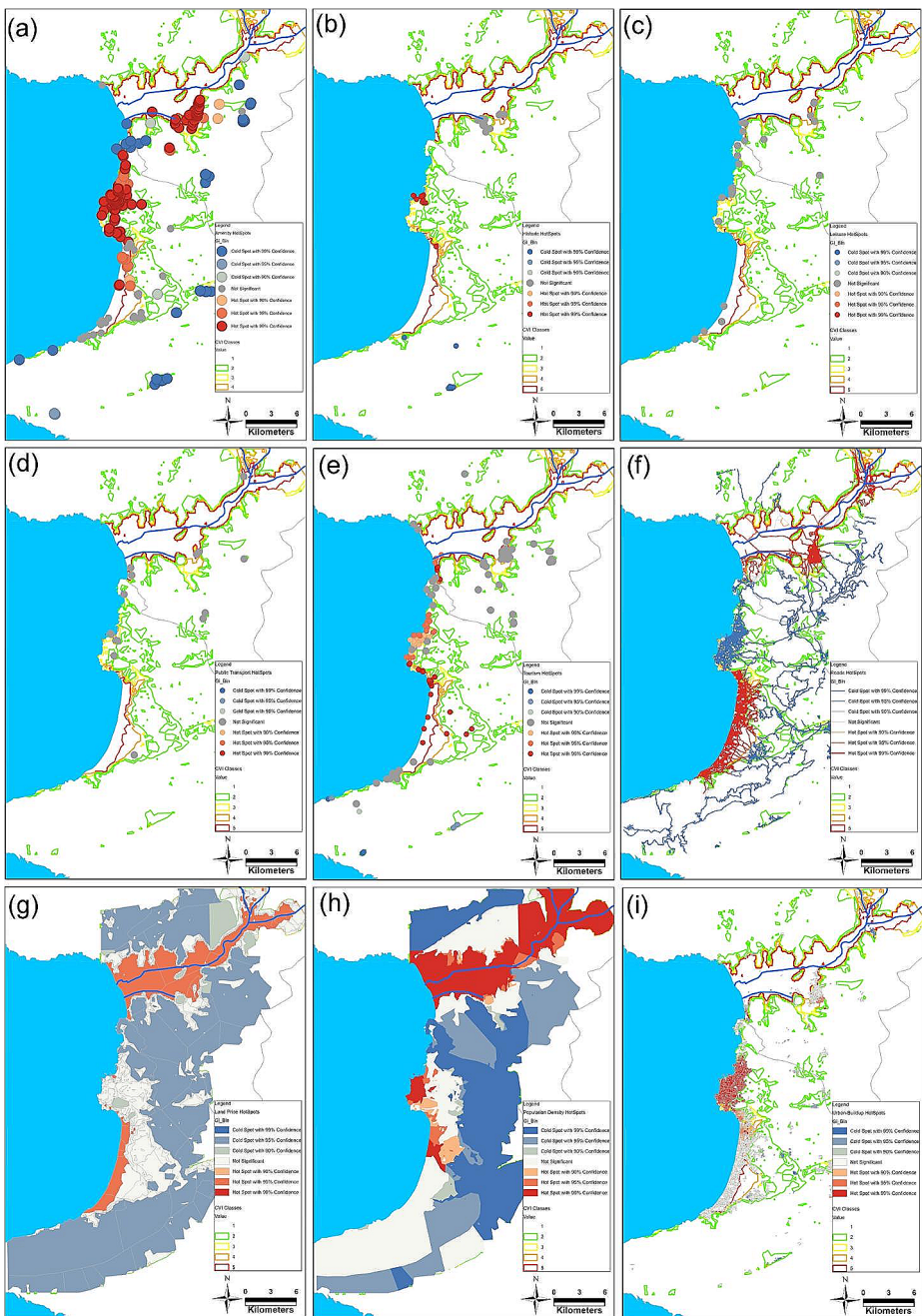


**Fig. 10** The distribution of infrastructures within areas with CVI values according to their statistical importance as hot point and cold point



Figure 10(f) shows areas where roads are vulnerable to coastal hazards. hot spots (red) highlight areas with high confidence, like Selcuk, Ephesus, Pamucak Beach, and the southern coast near Kusadasi. These areas likely have critical roads at risk. Cold spots (blue) around Kusadasi and inland areas show lower vulnerability. This suggests coastal roads near Selcuk and Pamucak Beach are more susceptible to coastal hazards.

Figure 10(g, h) shows areas vulnerable to coastal hazards due to high land value and population density. Hotspots (red) highlight areas with very high confidence, like Pamucak Beach, the Menderes Delta, and inland areas near the delta. These areas have both valuable land and high populations, making them potentially more susceptible. Coldspots (blue) inland show lower vulnerability due to lower land value and population density. This suggests a link between coastal proximity, valuable land, and high populations creating zones of greater vulnerability.

Figure 10(i) highlights coastal areas (red) with concentrated development, potentially vulnerable to coastal hazards (Selcuk, Kusadasi, and south Kusadasi). These areas are likely densely populated and have critical infrastructure, making them more susceptible. Inland areas (blue) show lower vulnerability due to lower development. This clustering suggests higher vulnerability along the coast due to concentrated populations and assets.

Hot spots warrant priority attention in coastal hazard adaptation strategies, as they represent areas with potentially high human and economic losses in the event of coastal events. Cold spots, while less vulnerable overall, may still require protective measures depending on specific contexts and projected hazard intensities.

*Recommendations for preparing adaptation strategies by using results; integrating multiple analyses for coastal infrastructure vulnerability adaptation strategy;* A Coastal Infrastructure Vulnerability Adaptation Strategy (CIVAS) for Kusadasi-Selcuk was recommended by integrating insights from three key analyses: Spatial Coastal Vulnerability Index (SCVI), Spatial Distribution of Infrastructure (SDI) within CVI Classes, and Hot Spot Distribution Analysis of Infrastructures. In this section, based on the results of these analyses, recommendations were presented for the preparation of adaptation strategies.

The IPCC report *Climate Change 2022: Impacts, Adaptation and Vulnerability* (IPCC, 2022) outlined various adaptation strategies for coastal infrastructure vulnerability. The report presented a comprehensive assessment of the current state of knowledge on the observed impacts and projected risks of climate change, as well as potential adaptation options but did not categorize them specifically for each infrastructure type.

Vulnerability assessment as one of the key considerations has been emphasized when selecting and implementing adaptation strategies for coastal infrastructure by this IPCC report. However, vulnerability assessment alone is not sufficient to prepare an effective and site-specific coastal infrastructure vulnerability adaptation strategy. Therefore, CIVAS for Kusadasi-Selcuk requires combining the insights from these three key analyses.

During the preparation of the CIVAS for the Kusadasi-Selcuk coastal region, the following questions arose regarding the utilization of analysis results: How to use the results of the Spatial Coastal Vulnerability Index (SCVI) analysis, the spatial distribution of infrastructure within SCVI classes, and the hot spot analysis of infrastructure distribution according to SCVI classes (with and without cluster)?

Using the Results of Spatial Coastal Vulnerability Index (SCVI) Analysis: The results of the SCVI analysis, which assesses the vulnerability of the coastal region, can be effectively utilized in the adaptation strategy. The vulnerability levels of different infrastructure types

can categorize as CVI-5, CVI-4, CVI-3, and CVI-2, and determine. These vulnerability levels provide valuable insights into the vulnerability of each infrastructure type to coastal hazards.

**Using the Results of Spatial Distribution of Infrastructure within SCVI Classes:** The spatial distribution of infrastructure within the SCVI classes offers crucial information for the adaptation strategy. By analysing this distribution, it is possible to identify areas with concentrated vulnerable infrastructure and prioritize adaptation efforts accordingly. Understanding the specific locations and concentrations of infrastructure within each vulnerability class enables tailored adaptation measures to be implemented effectively.

**Using the Results of Hot Spot Analysis:** The analysis of dispersed infrastructure in the hot spot analysis provides valuable insights for the adaptation strategy. Even though no distinct hot spots can be identified, the following key points can be considered:

- **Individual Vulnerability:** Each infrastructure element, regardless of its location, possesses its own vulnerability level. Understanding these individual vulnerabilities is crucial for developing appropriate adaptation strategies.
- **Cumulative Impact Assessment:** While individually less impactful, the combined vulnerabilities of dispersed infrastructure can create significant challenges. Assessing these cumulative impacts helps prioritize adaptation efforts.
- **Network Interdependency Analysis:** Infrastructure often functions as interconnected networks, even if physically dispersed. Analysing these network dependencies helps identify critical nodes and prioritize their protection.
- **Importance of Individual Infrastructure:** Even dispersed infrastructure can hold high individual importance due to its unique function. Protecting critical assets remains crucial in the adaptation strategy.
- **Multi-Scale Approach:** A multi-scale approach is necessary when dealing with dispersed infrastructure. Understanding regional trends and broader vulnerabilities helps plan for large-scale coastal processes and potential future changes. In addition, specific adaptation strategies summarized below can be recommended according to the vulnerability levels of different infrastructure types (CVI-5, CVI-4, CVI-3, CVI-2);

#### Build-up Infrastructure:

- Elevating beach access points, boardwalks, and recreational facilities.
- Implementing flood-proofing measures, such as flood barriers and elevating electrical systems.
- Choosing drought-resistant landscaping and native plants.
- Diversifying tourism offerings towards inland areas and promoting responsible tourism practices.

#### Natural Environment Infrastructure:

- Documenting and prioritizing cultural heritage sites for protection.
- Implementing protective measures, including flood barriers and shoreline stabilization.
- Considering relocation as a last resort, with proper documentation and potential reconstruction elsewhere.

Socio-economic Infrastructure:

- Elevating roads and railway lines in vulnerable areas.
- Constructing flood-resistant bridges and tunnels where necessary.
- Implementing early warning systems and evacuation plans for vulnerable transportation networks.
- Considering alternative routes or modes of transport for low-lying areas.

Tourism Infrastructure:

- Diversifying tourism offerings towards less vulnerable inland areas.
- Investing in eco-tourism practices that protect coastal ecosystems.
- Implementing measures to reduce water consumption and energy use in tourism facilities.

Urban and Built-up Areas:

- Implementing green infrastructure solutions, such as rain gardens and permeable pavements.
- Improving drainage systems and flood defences.
- Enforcing stricter building codes and land-use planning regulations.
- Elevating critical infrastructure like hospitals and emergency services.

Cropland:

- Choosing salt-tolerant crop varieties and adjusting agricultural practices.
- Implementing soil conservation measures, such as cover crops and terracing.
- Exploring options for managed retreat of agricultural land in severely affected areas.

Woodland and Forests, Grassland, Wetlands, etc.:

- Managing coastal ecosystems for their natural ability to buffer against storms and erosion.
- Considering nature-based solutions, such as planting salt marshes.

Water Infrastructure:

- Implementing water conservation measures to manage scarcity.
- Investing in desalination plants in water-scarce regions.
- Upgrading water treatment facilities to handle changes in salinity and storm runoff.

Thus, by integrating the results of SCVI analysis with the spatial distribution of infrastructure and hot spot analysis outcomes, stakeholders can develop comprehensive adaptation strategies tailored to address the varying levels of vulnerability and prioritize actions to safeguard critical coastal infrastructure from potential hazards.

## 5 Discussion

In this study, a new methodology integrating spatial coastal vulnerability index (CVI) and hot spot analysis was proposed for a comprehensive and holistic coastal infrastructure (natural, built-up and socioeconomic) vulnerability assessment and determination of its spatial distribution. For the assessment of coastal infrastructure vulnerability across the study area, coastal vulnerability level of each grid calculated using the CVI method. The spatial CVI analyses were performed by basic GIS methods (subset, buffer, slope, reclass, map algebra etc.). Natural (cropland, wetland etc.), built (coastal infrastructures such as ports, roads, tourism sites etc.), and socioeconomic (population density, land price etc.) infrastructures of study area were determined according to quality, quantity and location information and a geographical database was created. The spatial distribution of coastal vulnerabilities of different types of coastal infrastructures was obtained. Finally, the statistical reliability test of the distribution of the coastal infrastructures across the area with different vulnerability level was examined via hot spot Analyses, for the first time in this study. The analysis results, as detailed in the [results](#) section, revealed extensive areas with high to very high vulnerability. These areas were particularly concentrated around the Kucuk Menderes delta, Pamucak Beach, Selcuk town, and Ephesus Ancient City. Furthermore, the integration of socioeconomic data to the research demonstrated the significant potential impact on land assets and population density within these vulnerable zones.

As a result of the analysis it seen that areas with high to very high vulnerability are concentrated around Selcuk town, Ephesus Ancient City, Kusadasi district centre, Pamucak Beach, and the Kucuk Menderes delta. The Kucuk Menderes delta is under the influence of SLR up to the inner regions, approximately 22 km away on the land side. Over 55% of infrastructure falls within high or very high vulnerability classes. It is seen that 57% of the infrastructure in the build-up category, 59% of the natural environment, and more than 42% of the socio-economic infrastructure are located in areas falling into the high or very high vulnerability classes. Additionally, \$1.1 billion worth of land assets and a population of approximately 143,000 people are located in areas that fall into the high or very high vulnerability classes. Statistically significant clusters of high vulnerability for historical sites, tourism, roads, land value, population density, and urban areas were determined by hot spot analysis results.

The observed concentration of high vulnerability around the Kucuk Menderes delta concurred with established the literature of review for CVI and IPCC report (IPCC 2022), which emphasizes the vulnerability of low-lying deltaic regions to sea level rise due to their low elevation and gentle slopes ( Simav et al. 2013; Simav et al. 2015; Hamid et al. 2019; Anfusio et al. 2021; Nguyen et al. 2016; Kantamaneni et al. 2019). However, This study's integration of socio-economic data revealed a critical aspect: the vulnerability translates into significant potential risks for land assets and population density within the delta. This finding highlights the critical need to consider socio-economic factors alongside physical characteristics in vulnerability assessments, as emphasized by previous research (VanZomeren and Acevedo-Mackey 2019; Posen et al. 2023; Koks et al. 2023; Tragaki et al. 2018). This comprehensive approach allows for more informed decision-making regarding adaptation strategies and resource allocation. A review of the extant literature reveals a lack of hot spot analyses examining the spatial distribution of coastal infrastructure within the framework of CVI classifications. Nonetheless, Torresan et al. (2012) employed hot spot

analysis to delineate areas of heightened vulnerability to climate change and coastal hazards within the Northern Adriatic Sea region, though their focus was not on coastal infrastructure specifically.

Compared to studies relying solely on CVI (Hegde and Reju 2007; Pendleton et al. 2004; Pantusa et al. 2018; Koroglu et al. 2019), integration in this research of CVI, spatial analysis, and hot spot analysis provided a more nuanced understanding of vulnerability across different infrastructure types and locations.

While previous studies provided valuable insights for the broader Aegean coast (Hereher 2013; Chaparría and Peris 2021; Pantusa et al. 2018; Ružić et al. 2019), our research delved deeper by offering site-specific vulnerability assessments for individual infrastructure elements within Kusadasi-Selcuk. This multifaceted approach, unlike broader regional assessments, allowed us to achieve a level of granularity not previously achieved. For instance, while the CVI analysis identified general vulnerabilities in Selcuk town, Ephesus Ancient City, and Kusadasi district centre (CVI 4–5), the spatial distribution analysis revealed pockets of high vulnerability within these areas, even in locations with moderate CVI scores. This is exemplified by the concentration of vulnerable leisure facilities around Pamucak Beach, despite its moderate CVI (3). This granular understanding, further refined by hot spot analysis, pinpointed statistically significant clusters of highly vulnerable historical sites, tourism facilities, and roads in specific locations. These findings highlight the limitations of relying solely on CVI and underscore the value of our site-specific approach in identifying critical infrastructure at risk, even in seemingly less vulnerable areas. Furthermore, our detailed analysis pinpointed the specific vulnerabilities of critical infrastructure, such as vulnerable sections of historical sites vulnerable to erosion, enabling us to propose targeted nature-based solutions. This approach allows for highly localized adaptation measures that are more likely to be effective and sustainable.

While CVI analysis of a spatial area offers valuable regional insights, it may mask localized vulnerabilities within moderate-risk zones. In this research, identified infrastructure clusters with high vulnerability even within areas with moderate CVI scores, for example vulnerable sections of roads prone to flooding, or historical sites and leisure infrastructure. This granularity is crucial for crafting targeted adaptation strategies that go beyond broad assessments. The application of hot spot analysis provided statistically robust validation of the spatial distribution patterns of infrastructure vulnerability across different types (built-up, natural, and socioeconomic). This information can inform targeted interventions and prioritize adaptation efforts in these areas, potentially improving upon the broader-scale approaches often employed in traditional vulnerability assessments. Furthermore, the study introduced the concept of “no clusters,” “fragmented clusters,” and “densely clustered” vulnerability patterns, each requiring different adaptation strategies. Thus, the importance of network interdependency between infrastructures has emerged. With network interdependency, it is necessary to analyse how interconnected infrastructure networks work even if they are physically dispersed. Network interdependency analysis is a very important guide for identifying critical nodes (e.g. important transport links) and prioritizing their protection.

This study significantly advances coastal vulnerability assessment through several novel approaches. It utilizes a dynamic boundary tailored to the specific coastline, providing a more accurate picture of vulnerable zones. By considering all types of infrastructure (natural, built, and socio-economic) and their interactions, the study offers a comprehensive understanding of vulnerability. Additionally, it employs advanced statistical analysis and

pioneering hot spot analysis to strengthen confidence in the identified vulnerable areas and reveal valuable patterns in infrastructure vulnerability. Highlighting the importance of network interdependencies, the study emphasizes the need to protect critical nodes, even if physically dispersed. Furthermore, it integrates physical and socio-economic data for deeper insights and focuses specifically on coastal infrastructure vulnerability, informing crucial decisions. For instance, our analysis revealed that over \$1.1 billion worth of land assets and a population of 143,000 in Kusadasi-Selcuk are located in high or very high vulnerability zones. This highlights the critical need to consider socio-economic factors alongside physical characteristics when prioritizing adaptation strategies. Recognizing the vital role of localized context, the study emphasizes the importance of place-specific assessments and integrates socio-economic factors to tailor interventions and build resilience for local communities.

While this research provides some insights and perspectives into coastal infrastructure vulnerability and spatial distribution, it has also some limitations. Data availability restricted the analysis to infrastructure types like roads, buildings, and historical sites. Future studies could benefit from incorporating a wider range of elements, such as wastewater treatment plants, communication networks, and power grids. This would provide a more holistic understanding of infrastructure vulnerability and potential cascading effects during coastal hazards. The dynamic boundary definition used in this research may require further refinement in future applications, particularly as sea level rise projections evolve. For example, by incorporating dynamic elevation data and considering future land-use changes in the boundary definition process. This could enhance the adaptability and accuracy of the approach in the face of evolving sea level rise projections and coastal dynamics. Integrating multiple analyses offers a comprehensive assessment, but further site-specific evaluations may be needed. The analysis considers current infrastructure distribution and vulnerability, but future development trends should be incorporated for long-term planning. For example, by conducting detailed engineering assessments of critical infrastructure elements could be identified as highly vulnerable. This could provide a deeper understanding of their specific vulnerabilities and inform the development of tailored adaptation strategies.

## 6 Conclusion

In conclusion, an integrated novel methodology for assessing coastal infrastructure vulnerability was used in this study. This methodology integrated the spatial CVI analysis with comprehensive data on natural, built, and socioeconomic infrastructure in a coastal zone. Basic GIS methods and statistical techniques were employed to provide a detailed understanding of vulnerability patterns across the study area. The integration of socioeconomic data revealed the potential risks posed to land assets and population density within vulnerable zones. This finding underscored the importance of considering both physical and human dimensions in vulnerability assessments. Additionally, hot spot analysis was used to examine the spatial distribution of coastal infrastructure vulnerability, offered valuable insights for targeted interventions and adaptation strategies. By focusing on site-specific infrastructure vulnerability assessments within the Kusadasi-Selcuk region, the study provided a granular understanding of vulnerability across different infrastructure types and locations, going beyond broader regional assessments. This localized approach allowed for

the identification of critical infrastructure at risk, even in seemingly less vulnerable areas, and enabled the proposal of targeted adaptation measures. However, data availability constraints and the static nature of the CVI methodology were highlighted as limitations of the study. Future research could benefit from incorporating a wider range of infrastructure elements and adopting more dynamic approaches to define study areas and assess vulnerability. Nonetheless, it is thought that this study can make significant contributions to the field of coastal infrastructure vulnerability assessment by providing innovative methodologies and insights that can support policy-making and resilience-building efforts in coastal areas.

**Author contributions** All authors contributed to the study's conception and design. Material preparation, data collection and analysis were performed by Tuncay Kuleli and Seyma Bayazit. The first draft of the manuscript was written by Tuncay Kuleli and all authors commented on previous versions of the manuscript. All authors read and approved the final manuscript.

**Funding** The authors declare that no funds, grants, or other support were received during the preparation of this manuscript.

Open access funding provided by the Scientific and Technological Research Council of Türkiye (TÜBİTAK).

## Declarations

**Competing Interests** The authors have no relevant financial or non-financial interests to disclose.

**Open Access** This article is licensed under a Creative Commons Attribution 4.0 International License, which permits use, sharing, adaptation, distribution and reproduction in any medium or format, as long as you give appropriate credit to the original author(s) and the source, provide a link to the Creative Commons licence, and indicate if changes were made. The images or other third party material in this article are included in the article's Creative Commons licence, unless indicated otherwise in a credit line to the material. If material is not included in the article's Creative Commons licence and your intended use is not permitted by statutory regulation or exceeds the permitted use, you will need to obtain permission directly from the copyright holder. To view a copy of this licence, visit <http://creativecommons.org/licenses/by/4.0/>.

## References

- Abuodha PAO, Woodroffe CD (2010) Assessing vulnerability to sea-level rise using a coastal sensitivity index: a case study from southeast Australia. *J Coast Conserv* 14:189–205. <https://doi.org/10.1007/s11852-010-0097-0>
- Akbaş B, Akdeniz N, Aksay A, Altun İE, Balcı V, Bilginer E, Bilgiç T, Duru M, Ercan T, Gedik İ, Günay Y, Güven İH, Hakyemez HY, Konak N, Papak İ, Pehlivan Ş, Sevin M, Şenel M, Tarhan N, Turhan N, Türkecan A, Ulu Ü, Uğuz MF, Yurtsever AT (2011) 1:1.250.000 scaled Geological Map of Turkey. General Directorate of Mineral Research and Exploration Publication, Ankara-Turkey. <http://yerbilimleri.mta.gov.tr/references.aspx>
- Anfuso G, Postacchini M, Di Luccio D, Benassai G (2021) Coastal sensitivity/vulnerability characterization and adaptation strategies: a review. *J Mar Sci Eng* 9(1):72. <https://doi.org/10.3390/jmse9010072>
- Beeharry YD, Bekaroo G, Bokhoree C et al (2022) Impacts of sea-level rise on coastal zones of Mauritius: insights following calculation of a coastal vulnerability index. *Nat Hazards* 114:27–55. <https://doi.org/10.1007/s11069-022-05378-9>
- Behera R, Kar A, Das MJ, Panda PP (2019) GIS-based vulnerability mapping of the coastal stretch from Puri to Konark in Odisha using analytical hierarchy process. *Nat Hazards* 96(3):731–751. <https://doi.org/10.1007/s11069-018-03566-0>
- Boruff BJ, Emrich C, Cutter SL (2005) Erosion hazard vulnerability of US coastal counties. *Journal of Coastal Research*, 21(5), 932–942. West Palm Beach (Florida): ISSN 0749–0208
- Bukvic A, Rohat G, Apotsos A, de Sherbinin A (2020) A systematic review of coastal vulnerability mapping. *Sustainability* 12(7):2822 MDPI AG. <https://doi.org/10.3390/su12072822>

- Caldwell PC, Merrfield MA, Thompson PR (2015) Sea level measured by tide gauges from global oceans - the Joint Archive for Sea Level holdings (NCEI Accession 0019568), Version 5.5 [Data set]. National Oceanic and Atmospheric Administration National Centers for Environmental Information. <https://doi.org/10.7289/v5v40s7w>
- Chaparría VE, Peris JS (2021) Vulnerability of coastal areas due to infrastructure: the case of Valencia Port (Spain). *Land* 10(12):1344. <https://doi.org/10.3390/land10121344>
- Charuka B, Angnuureng DB, Brempong EK, Agblorti SKM, Agyakwa KTA (2023) Assessment of the integrated coastal vulnerability index of Ghana toward future coastal infrastructure investment plans. *Ocean Coastal Manage* 244:106804. <https://doi.org/10.1016/j.ocecoaman.2023.106804>
- CMS (Copernicus Marine Service) (2022) Global Ocean Waves Reanalysis WAVERYS. Retrieved November 29, from <https://doi.org/10.48670/moi-00022>
- CMS (Copernicus Marine Service), In Situ TAC Data Management Team (2021) Copernicus Marine (2021). Copernicus Marine in situ TAC - physical parameters list. Retrieved November 29, from <https://doi.org/10.13155/53381>
- CORINE (2018) Copernicus Marine Environment Monitoring Service (CMEMS). CORINE Coastal Zones 2018 Map. Product background, Product evolution. <https://land.copernicus.eu/local/coastal-zones>. Retrieved from <https://land.copernicus.eu/local/coastal-zones/coastal-zones-2018>
- Dey J, Mazumder S (2023) Development of an integrated coastal vulnerability index and its application to the low-lying Mandarmani-Dadanpatrabar coastal sector, India. *Nat Hazards* 116:3243–3273. <https://doi.org/10.1007/s11069-022-05805-x>
- Djouder F, Boutiba M (2017) Vulnerability assessment of coastal areas to sea level rise from the physical and socioeconomic parameters: case of the Gulf Coast of Bejaia, Algeria. *Arab J Geosci* 10:1–20. <https://doi.org/10.1007/s12517-017-3062-5>
- ECU (Ecological Coastal Units) (2022) 1km global shoreline segments and segment midpoints characterized and clustered. Retrieved on November 29, 2023 from <https://www.arcgis.com/home/item.html?id=b3920b9e386945f2942e72e38f9142fe>
- ESA (2023) Copernicus Sentinel-2 (processed by ESA), 2021, MSI Level-2A BOA Reflectance Product. Collection 1. European Space Agency. [https://doi.org/10.5270/S2\\_-zmk9xsj](https://doi.org/10.5270/S2_-zmk9xsj)
- Esri (2023a) How hot spot analysis (Getis-Ord Gi\*) works. ArcGIS Pro 3.2 Help. Release Date: 11/7/2023. Retrieved November 10, 2023 from <https://pro.arcgis.com/en/pro-app/latest/tool-reference/spatial-statistics/h-how-hot-spot-analysis-getis-ord-gi-spatial-stati.htm>
- Esri (2023b) Hot spot analysis (Getis-Ord Gi\*) (spatial statistics). ArcGIS Pro 3.2 Help. Release Date: 11/7/2023. Retrieved November 10, 2023 from <https://m.youtube.com/watch?v=7N7ejOJxULY>
- Fernandez-Macho J, Gonzalez P, Virdo J (2020) Assessing anthropogenic vulnerability of coastal regions: DEA-based index and rankings for the European Atlantic Area, *Marine Policy* 119 (2020) 104030
- Getis A, Ord JK (1992) The Analysis of Spatial Association by Use of Distance statistics. *Geographical Anal* 24:189–206. <https://doi.org/10.1111/j.1538-4632.1992.tb00261.x>
- Getis A, Ord JK (2010) The Analysis of Spatial Association by Use of Distance statistics. In: Anselin L, Rey S (eds) *Perspectives on spatial data analysis*. Advances in Spatial Science. Springer, Berlin, Heidelberg. [https://doi.org/10.1007/978-3-642-01976-0\\_10](https://doi.org/10.1007/978-3-642-01976-0_10)
- Gornitz V (1990) Vulnerability of the East Coast, USA to future sea level rise. *J Coastal Res Special Issue No 9*:201–237
- Gornitz V (1991) Global coastal hazards from future sea level rise. *Palaeogeogr Palaeoclimatol Palaeoecol* 89:379–398. [http://refhub.elsevier.com/S0964-5691\(18\)30877-9/sref32](http://refhub.elsevier.com/S0964-5691(18)30877-9/sref32)
- Gornitz V, White T (1992) A coastal hazards database for the U.S. East Coast. ORNL/CDIAC-45, NDP-043 A. Oak Ridge National Laboratory, Oak Ridge, Tennessee, U.S. August 1992
- Gornitz V, Daniels RC, White TW, Birdwell KR (1994) The development of a coastal risk assessment database: vulnerability to sea-level rise in the U.S. southeast. *J Coastal Res Special Issue No 12*:327–338
- Gzam M, Mansouri B, Gargouri D et al (2022) Assessment of the Coastal Sensitivity in the Southern Mediterranean using the CSI. *Environ Process* 9:39. <https://doi.org/10.1007/s40710-022-00584-w>
- Hamid AIA, Din AHM, Yusof N, Abdulllah NM, Omar AH, Abdull Khanan MF (2019) Coastal vulnerability index development: a review. *Int Archives Photogrammetry Remote Sens Spat Inform Sci* 42(4/W16):229–235. <https://doi.org/10.5194/isprs-archives-XLII-4-W16-229-2019>
- Hastuti AW, Nagai M, Suniada KI (2022) Coastal Vulnerability Assessment of Bali Province, Indonesia using remote sensing and GIS approaches. *Remote Sens* 14:4409. <https://doi.org/10.3390/rs14174409>
- Hegde AV, Reju VR (2007) Development of coastal vulnerability index for Mangalore coast, India. *J Coastal Res* 23(5):1106–1111. <https://doi.org/10.2112/04-0259.1>
- Hereher ME (2013) Coastal vulnerability assessment for Egypt's Mediterranean coast. *Geomatics Nat Hazards Risk* 6(4):342–355. <https://doi.org/10.1080/19475705.2013.845115>



- Himmelstoss EA, Henderson RE, Kratzmann MG, Farris AS (2021) Digital Shoreline Analysis System (DSAS) version 5.1 user guide. U S Geol Surv Open-File Rep 2021 – 1091 104. <https://doi.org/10.3133/ofr20211091>
- IPCC, Contribution of Working Group I to the Sixth Assessment Report of the Intergovernmental Panel on Climate Change [Masson-Delmotte V (2021) Climate Change 2021: The Physical Science Basis., P Zhai, A Pirani, SL Connors, C Péan, S Berger, N Caud, Y Chen, L Goldfarb, MI Gomis, M Huang, K Leitzell, E Lonnoy, JBR Matthews, TK Maycock, T Waterfield, O Yelekçi, R Yu, and B Zhou (eds.)]. Cambridge University Press, Cambridge, United Kingdom and New York, NY, USA. In press, <https://doi.org/10.1017/9781009157896>
- IPCC, Contribution of Working Group II to the Sixth Assessment Report of the Intergovernmental Panel on Climate Change [H-O (2022) Climate Change 2022: Impacts, Adaptation, and Vulnerability. Pörtner, DC Roberts, M. Tignor, ES Poloczanska, K Mintenbeck, A Alegría, M Craig, S Langsdorf, S Löschke, V Möller, A Okem, B Rama (eds.)]. Cambridge University Press. Cambridge University Press, Cambridge, UK and New York, NY, USA, 3056 pp., <https://doi.org/10.1017/9781009325844>
- IPCC (2023) Summary for Policymakers. In: Climate Change 2023: Synthesis Report. Contribution of Working Groups I, II and III to the Sixth Assessment Report of the Intergovernmental Panel on Climate Change [Core Writing Team, H Lee and J Romero (eds.)]. IPCC, Geneva, Switzerland, pp. 1–34, <https://doi.org/10.59327/IPCC/AR6-9789291691647.001>
- Kahraman C (2011) Land use and problems in Kusadasi Bay coastal areas. [Ph.D. Dissertation, Istanbul University, Institute of Social Sciences, Department of Geography, Istanbul]
- Kantamaneni K (2016) Coastal infrastructure vulnerability: an integrated assessment model. *Nat Hazards* (2016) 84:139–154. <https://doi.org/10.1007/s11069-016-2413-y>
- Kantamaneni K, Sudha Rani NV, Rice L, Sur K, Thayaparan M, Kulatunga U, Rege R, Yenneti K, Campos LC (2019) A systematic review of coastal vulnerability assessment studies along Andhra Pradesh, India: a critical evaluation of data gathering, risk levels and mitigation strategies. *Water* 11:393. <https://doi.org/10.3390/w11020393>
- KCoC (Kusadasi Chamber of Commerce) (2015) Seçilmiş Göstergelerle Kuşadası Ekonomisi. Retrieved from <https://kuto.org.tr/raporlar/> (Accessed: August 28, 2023)
- Koks EE, Le Bars D, Essenfelder AH, Nirandjan S, Sayers P (2023) The impacts of coastal flooding and sea level rise on critical infrastructure: a novel storyline approach. *Sustainable Resilient Infrastructure* 8(sup1):237–261. <https://doi.org/10.1080/23789689.2022.2142741>
- Koroglu A, Ranasinghe R, Jiménez JA, Dastgheib A (2019) Comparison of Coastal Vulnerability Index applications for Barcelona Province. *Ocean Coastal Manage* 178:104799. <https://doi.org/10.1016/j.ocecoaman.2019.05.001>
- Kovaleva O, Sergeev A, Ryabchuk D (2022) Coastal vulnerability index as a tool for current state assessment and anthropogenic activity planning for the Eastern Gulf of Finland coastal zone (the Baltic Sea). *Appl Geogr* 143(2022):102710
- Kuleli T (2010) *Estuaries Coasts* 33(3):640–651. <https://doi.org/10.1007/s12237-009-9248-7>. City-based risk assessment of sea level rise using topographic and census data for the Turkish Coastal zone
- Kusadasi Port (2023) Ege Port Kusadasi, General information. Retrieved from <https://www.kusadasicruise-port.com/general-information> (Accessed: August 25, 2023)
- Lewsey C, Cid G, Kruse E (2004) Assessing climate change impacts on coastal infrastructure in the Eastern Caribbean. *Mar Policy* 28(2004):393–409
- Lopes NDR, Li T, Matomela N, Sa RM (2022) Coastal vulnerability assessment based on multi-hazards and bio-geophysical parameters. case study – Northwestern coastline of Guinea-Bissau, *Natural Hazards* (2022) 114:989–1013, <https://doi.org/10.1007/s11069-022-05420-w>
- Lopez RM, Ranasinghe R, Jiménez JA (2016) A rapid, low-cost approach to coastal vulnerability assessment at a national level. *J. Coast. Res.* 32 (4), 932–945. [http://refhub.elsevier.com/S0964-5691\(18\)30877-9/sref51](http://refhub.elsevier.com/S0964-5691(18)30877-9/sref51)
- Mani Murali R, Ankita M, Amrita S, Vethamony P (2013) Coastal vulnerability assessment of Puducherry coast, India, using the analytical hierarchical process. *Nat Hazards Earth Syst Sci* 13:3291–3311. <https://doi.org/10.5194/nhess-13-3291-2013>
- Meddah RY, Ghodbani T, Senouci R, Rabehi W, Duarte L, Teodoro AC (2023) Estimation of the Coastal Vulnerability Index using Multi-criteria decision making: the Coastal Social-Ecological System of Rachoun. *Western Algeria Sustain* 15:12838. <https://doi.org/10.3390/su151712838>
- Minunno R, Andersson N, Morrison GM (2023) A systematic literature review considering the implementation of planetary geoengineering techniques for the mitigation of sea-level rise. *Earth Sci Rev* 241:104431. <https://doi.org/10.1016/j.earscirev.2023.104431>
- MoCT (Ministry of Culture and Tourism) (2023) Izmir Provincial Directorate of Culture and Tourism. Accommodation facilities. Retrieved from <https://izmir.ktb.gov.tr/TR-77418/efes-selcuk.html> (Accessed: August 29, 2023)

- MoEUCC (Ministry of Environment, Urbanization, and Climate Change) (2023) Population density, area (km<sup>2</sup>) of Kusadasi. Retrieved from <https://aydin.csb.gov.tr/ilceleri-i-1112> (Accessed: August 25, 2023)
- Mullick MRA, Tanim AH, Islam SMS (2019) Coastal vulnerability analysis of Bangladesh coast using fuzzy logic-based geospatial techniques. *Ocean Coastal Manage* 174:154–169. <https://doi.org/10.1016/j.ocecoaman.2019.03.010>
- NASA JPL (National Aeronautics and Space Administration Jet Propulsion Laboratory) (2013) NASA Shuttle Radar Topography Mission Global 1 arc second number [Data set]. NASA EOSDIS Land Processes DAAC. Retrieved on November 29, 2022 from <https://doi.org/10.5067/MEaSURES/SRTM/SRTMGLIN.003>
- Nazarnia H et al (2020) A systematic review of civil and environmental infrastructures for coastal adaptation to sea level rise. *Civ Eng J* 6(7):1375–1399. <https://doi.org/10.28991/cej-2020-03091555>
- Neumann B, Vafeidis AT, Zimmermann J, Nicholls RJ (2015) Future Coastal Population growth and exposure to sea-level rise and Coastal flooding - A Global Assessment. *PLoS ONE* 10(3):e0118571. <https://doi.org/10.1371/journal.pone.0118571>
- Nguyen TX, Thang PQ, Bonetti J, Rogers K, Woodroffe CD (2016) Indicator-based assessment of climate-change impacts on coasts: a review of concepts, methodological approaches and vulnerability indices. *Ocean Coastal Manage* 123:18–43. <https://doi.org/10.1016/j.ocecoaman.2015.11.022>
- Ord JK, Getis A (1995) Local spatial Autocorrelation statistics: Distributional issues and an application. *Geographical Anal* 27:286–306. <https://doi.org/10.1111/j.1538-4632.1995.tb00912.x>
- Özhan E, Abdalla S (2002) Türkiye kıyıları rüzgar ve derin deniz dalga atlası. *MedCoast – Orta Doğu Teknik Üniversitesi, Sürüm 1.0, 2002*, ISBN: 975429190X, 9789754291902 445 s. [Turkey coast wind and deep sea wave atlas. *MedCoast – Middle East Technical University, Version 1.0, 2002*, ISBN: 975429190X, 9789754291902, 445 p.]
- Pantusa D, D'Alessandro F, Riefolo L, Principato F, Tomasicchio GR (2018) Application of a coastal vulnerability index: a case study along the apulian coastline. *Italy Water* 10:1218. <https://doi.org/10.3390/w10091218>
- Pendleton EA, Williams SJ, Thieler ER (2004) Coastal vulnerability assessment of Assateague Island National Seashore (ASIS) to sea-level rise. U.S. Geological Survey, Open-File Report 2004–1020. ISSN: 2331–1258 (online)
- Pesaresi M, Politis P, GHS-BUILT-S (2023) R2023A - GHS built-up surface grid, derived from Sentinel2 composite and Landsat, Multitemporal (1975–2030). European Commission, Joint Research Centre (JRC). Retrieved from [https://ghsl.jrc.europa.eu/ghs\\_buS2023.php](https://ghsl.jrc.europa.eu/ghs_buS2023.php)
- Pethick JS, Crooks S (2000) Development of a coastal vulnerability index: a geomorphological perspective. *Environ Conserv* 27(4):359–367. <https://doi.org/10.1017/S0376892900000412>
- Posen PE, Beraud C, Harper Jones C, Tyllianakis E, Joseph-Witzig A, Louis S, A (2023) Vulnerability of coastal infrastructure and communities to extreme storms and rising sea levels: an improved model for Grenada and its dependencies. *Land* 12(7):1418. <https://doi.org/10.3390/land12071418>
- Ramieri E, Hartley A, Barbanti A, Duarte Santos F, Gomes A, Hilden M, Laihonon P, Marinova N, Santini M (2011) Methods for assessing coastal vulnerability to climate change. European topic centre on climate change impacts, vulnerability and adaptation (ETC/CCA). Technical paper, Bologna (IT) 93, October, 2011
- Rani NNV, Satyanarayana ANV, Bhaskaran PK (2015) Coastal vulnerability assessment studies over India: a review. *Nat Hazards* 77(1):405–428. <https://doi.org/10.1007/s11069-015-1597-x>
- Roukounis CN, Tsoukala VK, Tsihrintzis VA (2023) An index-based method to assess the resilience of Urban Areas to Coastal flooding: the case of Attica, Greece. *J Mar Sci Eng* 11(1776). <https://doi.org/10.3390/jmse11091776>
- Ružić I, Dugonjić Jovančević S, Benac Č, Krvavica N (2019) Assessment of the coastal vulnerability index in an area of complex geological conditions on the Krk Island. *Northeast Adriatic Sea Geosci* 9(5):219. <https://doi.org/10.3390/geosciences9050219>
- Sarkar N, Rizzo A, Vandelli V, Soldati M (2022) A Literature Review of Climate-Related Coastal Risks in the Mediterranean, a Climate Change Hotspot. *Sustainability* 2022, 14, 15994. <https://doi.org/10.3390/su142315994>
- Sayre R et al (2018) A new 30 meter resolution global shoreline vector and associated global islands database for the development of standardized global ecological coastal units. *J Oper Oceanogr – A*. <https://doi.org/10.1080/1755876X.2018.1529714>. Special Blue Planet Edition
- Sayre R, Butler K, VanGraafeiland S, Breyer D, Wright C, Frye D et al (2021) Earth's coastlines. In: Wright D, Harder C (eds) *GIS for Science, volume 3: maps for saving the planet*. Esri, Redlands, California. <https://pubs.er.usgs.gov/publication/70222519>
- SCoC (Selcuk Chamber of Commerce) (2016) Turizm Sektör Raporu. Retrieved from <https://www.selcukticaretodasi.org.tr/yayinlar/ekonomik-raporlar/819/> (Accessed: August 28, 2023)

- Selcuk Ekonomik Profili, SCoC (Selcuk Chamber of Commerce), Raporu D (2015) Ekim 2015. Retrieved from <https://www.selcukticaretodasi.org.tr/yayinlar/ekonomik-raporlar/819/> (Accessed: August 28, 2023)
- Shaw J, Taylor RB, Forbes DL, Ruz MH, Solomon S (1998) Sensitivity of the coasts of Canada to Sea-Level rise. *Geol Surv Can* 505:1–79. <https://doi.org/10.4095/210075>
- Shen S, Feng X, Peng ZR (2016) A framework to analyze vulnerability of critical infrastructure to climate change: the case of a coastal community in Florida. *Natural Hazards*, 84, 589–609 (2016). <https://doi.org/10.1007/s11069-016-2442-6>
- Šimac Z, Lončar N, Faivre S (2023) Overview of Coastal Vulnerability indices with reference to physical characteristics of the Croatian Coast of Istria. *Hydrology* 10:14. <https://doi.org/10.3390/hydrology10010014>
- Simav O, Seker DZ, Gazioglu C (2013) Coastal inundation due to sea level rise and extreme sea state and its potential impacts: Çukurova Delta case. *Turkish J Earth Sci* 22(4):11. <https://doi.org/10.3906/yer-1205-3>
- Simav O, Seker DZ, Tanik A, Gazioglu C (2015) Determining the endangered fields of Turkish coasts with coastal vulnerability index. *J Map* 153:1–8
- SLE (The Sea Level Explorer) (2022) Satellite altimetry and tide gauge data for exploring sea level changes and measurement comparisons. Retrieved on November 29, 2022, from <https://ccar.colorado.edu/altimetry/index.html>
- SRTM (Shuttle Radar Topography Mission) (2018) 1 Arc-Second Global elevation data offer worldwide coverage of void filled data at a resolution of 1 arc-second (30 meters) and provide open distribution of this high-resolution global data set. Retrieved on November 29, 2022, from <https://doi.org/10.5066/F7PR7TFT>
- Tang HS et al (2013) Vulnerability of population and transportation infrastructure at the east bank of Delaware Bay due to coastal flooding in sea-level rise conditions. *Nat Hazards* 69:141–163
- Thieler ER, Hammar-Klose (1999) National Assessment of Coastal vulnerability to Future Sea-Level rise: preliminary results for the U.S. Atlantic Coast. U.S. Geological Survey, Open-File Rep 99–593, 1 sheet
- Thieler ER, Hammar-Klose (2000) National Assessment of Coastal Vulnerability to Future Sea-Level Rise: Preliminary Results for the U.S. Pacific Coast: U.S. Geological Survey, Open-File Report 00-178. [http://refhub.elsevier.com/S0964-5691\(18\)30877-9/sref78](http://refhub.elsevier.com/S0964-5691(18)30877-9/sref78)
- Torresan S, Critto A, Dalla Valle M et al (2008) Assessing coastal vulnerability to climate change: comparing segmentation at global and regional scales. *Sustain Sci* 3:45–65. <https://doi.org/10.1007/s11625-008-0045-1>
- Torresan S, Critto A, Rizzi J, Marcomini A (2012) Assessment of coastal vulnerability to climate change hazards at the regional scale: the case study of the North Adriatic Sea. *Nat Hazards Earth Syst Sci* 12:2347–2368. <https://doi.org/10.5194/nhess-12-2347-2012>
- Tragaki A, Gallousi C, Karymbalis E (2018) Coastal hazard vulnerability assessment based on geomorphic, oceanographic and demographic parameters: the case of the Peloponnese (Southern Greece). *Land* 7(2):56. <https://doi.org/10.3390/land7020056>
- TUDES (Türkiye Ulusal Deniz Seviyesi İzleme Sistemi) (2022) Sea Level Observations. Retrieved on November 29, 2022 from <https://tudes.harita.gov.tr/>
- TURKSTAT (Turkish Statistical Institute) (2023) Population census. Retrieved from <https://data.tuik.gov.tr/Bulten/Index?p=49685> (Accessed: August 29, 2023)
- VanZomeren C, Acevedo-Mackey D (2019) A review of coastal vulnerability assessments: Definitions, components, and variables (Special Report (Engineer Research and Development Center (U.S.)); no. ERDC/EL SR-19-5). Engineer Research and Development Center (U.S.). <https://erdclibrary.erdcdren.mil/jspui/handle/11681/33289>
- Vernimmen R, Hooijer A (2023) New LiDAR-based elevation model shows greatest increase in global coastal exposure to flooding to be caused by early-stage sea-level rise. *Earth's Future*, 11, e2022EF002880. <https://doi.org/10.1029/2022EF002880>
- Wang Y, Marsooli R (2021) Dynamic modelling of sea-level rise impact on coastal flood hazard and vulnerability in New York City's built environment. *Coastal Engineering* 169 (2021) 103980
- Young JD (2022) Forest measurements: an applied approach. Publisher Open or Educational Resour Ebook ISBN 978-1-63635-053-0 Retrieved on November 29
- Zhao Q, Pan J, Devlin AT, Tang M, Yao C, Zamparelli V, Falabella F, Pepe A (2022) On the Exploitation of Remote Sensing Technologies for the Monitoring of Coastal and River Delta Regions. *Remote Sens.* 2022, 14, 2384. <https://doi.org/10.3390/rs14102384>
- Zlotnicki V, Qu Z, Joshua W (2019) MEaSURES Gridded Sea Surface Height Anomalies Version 1812. Ver. 1812. PO.DAAC, CA, USA. <https://doi.org/10.5067/SLREF-CDRV2>